"ROLE OF DIFFUSION WEIGHTED MRI IN DIFFERENTIATING BENIGN FROM MALIGNANT THYROID NODULES"

By

Dr. MONISHA V.

DISSERTATION SUBMITTED TO SRI DEVARAJ URS ACADEMY OF HIGHER EDUCATION AND RESEARCH, KOLAR, KARNATAKA

In partial fulfilment of the requirements for the degree of

DOCTOR OF MEDICINE
IN
RADIODIAGNOSIS

Under the Guidance of

Dr. N. RACHEGOWDA, MBBS , MD , DMRD
PROFESSOR,
DEPT. OF RADIO-DIAGNOSIS

DEPARTMENT OF RADIODIAGNOSIS,
SRI DEVARAJ URS MEDICALCOLLEGE,
TAMAKA, KOLAR-563101

2022

SRI DEVARAJ URS ACADEMY OF HIGHER EDUCATION AND RESEARCH, TAMAKA, KOLAR, KARNATAKA

DECLARATION BY THE CANDIDATE

I hereby declare that this dissertation entitled **"ROLE OF DIFFUSION WEIGHTED MRI IN DIFFERENTIATING BENIGN FROM MALIGNANT THRYOID NODULES"** is a bonafide and genuine research work carried out by me under the guidance of **Dr. N. RACHEGOWDA**, Professor, Department of Radiodiagnosis, Sri Devaraj Urs Medical College, Kolar, in partial fulfilment of University regulation for the award "**M. D. DEGREE IN RADIODIAGNOSIS**", the examination to be held in 2022 by SDUAHER. This has not been submitted by me previously for the award of any degree or diploma from the university or any other university.

Date:

Dr. MONISHA V.
Postgraduate in Radiodiagnosis
Sri Devaraj Urs Medical College
Tamaka, Kolar.

SRI DEVARAJ URS ACADEMY OF HIGHER EDUCATIONAND RESEARCH, TAMAKA, KOLAR, KARNATAKA

CERTIFICATE BY THE GUIDE

This is to certify that the dissertation entitled "**ROLE OF DIFFUSION WEIGHTED MRI IN DIFFERENTIATING BENIGN FROM MALIGNANT THRYOID NODULES"** is a bonafide research work done by **Dr. MONISHA V.,** under my direct guidance and supervision at Sri Devaraj Urs Medical College, Kolar**,** in partial fulfilment of the requirement for the degree of "**M.D. IN RADIODIAGNOSIS"**.

Date:

Place: Kolar

Dr. N. RACHEGOWDA, **MBBS, MD, DMRD**

Professor,

Department Of Radiodiagnosis

Sri Devaraj Urs Medical College

Tamaka, Kolar

SRI DEVARAJ URS ACADEMY OF HIGHER EDUCATION

AND RESEARCH, TAMAKA, KOLAR, KARNATAKA

CERTIFICATE BY THE HEAD OF DEPARTMENT

This is to certify that the dissertation entitled **"ROLE OF DIFFUSION WEIGHTED MRI IN DIFFERENTIATING BENIGN FROM MALIGNANT THRYOID NODULES"** is a bonafide research work done by **Dr. MONISHA V.,** under my supervision at Sri Devaraj Urs Medical College, Kolar**,** in partial fulfilment of the requirement for the degree of "**M.D. IN RADIODIAGNOSIS"**.

Date:

Place: Kolar

Dr. ANIL KUMAR SAKALECHA, **MBBS, MD**

Professor & HOD

Department Of Radiodiagnosis

Sri Devaraj Urs Medical College

Tamaka, Kolar.

SRI DEVARAJ URS ACADEMY OF HIGHER EDUCATION AND RESEARCH, TAMAKA, KOLAR, KARNATAKA

ENDORSEMENT BY THE HEAD OF THE DEPARTMENT AND PRINCIPAL

This is to certify that the dissertation entitled, **"ROLE OF DIFFUSION WEIGHTED MRI IN DIFFERENTIATING BENIGN FROM MALIGNANT THRYOID NODULES"** is a bonafide research work done by **Dr. MONISHA V.** under the direct guidance and supervision of **Dr. N. RACHEGOWDA,** Professor, Department of Radiodiagnosis, Sri Devaraj Urs Medical College, Kolar, in partial fulfilment of University regulation for the award "**M.D. DEGREE IN RADIODIAGNOSIS**".

Dr.ANIL KUMAR SAKALECHA	**DR. P.N. SREERAMULU**
Professor & HOD	Principal,
Department Of Radiodiagnosis,	Sri Devaraj Urs Medical College,
Sri Devaraj Urs Medical College,	Tamaka,
Tamaka, Kolar.	Kolar.
Date:	Date:
Place: Kolar	Place: Kolar

SRI DEVARAJ URS ACADEMY OF HIGHER EDUCATION

AND RESEARCH TAMAKA, KOLAR, KARNATAKA

ETHICAL COMMITTEE CERTIFICATE

This is to certify that the Ethical committee of Sri Devaraj Urs Medical College,

Tamaka,Kolar has unanimously approved

Dr. MONISHA V.

Post-Graduate student in the subject of

RADIODIAGNOSIS at Sri Devaraj Urs Medical College, Kolar

to take up the Dissertation work entitled

"ROLE OF DIFFUSION WEIGHTED MRI IN DIFFERENTIATING BENIGN FROM MALIGNANT THRYOID NODULES"

to be submitted to the

SRI DEVARAJ URS ACADEMY OF HIGHER EDUCATION AND

RESEARCH, TAMAKA, KOLAR, KARNATAKA.

Signature of Member Secretary
Ethical Committee
Date :
Place : Kolar

Signature of Principal
Dr. P.N. SREERAMULU
Sri Devaraj Urs Medical College
Kolar, Karnataka

SRI DEVARAJ URS ACADEMY OF HIGHER EDUCATION AND RESEARCH TAMAKA, KOLAR, KARNATAKA

COPY RIGHT DECLARATION BY THE CANDIDATE

I hereby declare that Sri Devaraj Urs Academy of Higher Education and Research, Kolar, Karnataka shall have the rights to preserve, use and disseminate this dissertation/thesis in print or electronic format for academic/research purpose.

Date :

Place : Kolar

Dr. MONISHA V.
Postgraduate
Department of Radio-diagnosis
Sri Devaraj Urs Medical College
Tamaka, Kolar

ACKNOWLEDGEMENT

I owe debt and gratitude to my parents ***Dr. S.N VIJAYA KUMAR.*** *and* ***Dr. C. POORNIMA****, along with my sister* ***Miss. VARSHA V.*** *for their moral support and constant encouragement during the study.*

With humble gratitude and great respect, I would like to thank my teacher, mentor and guide, ***Dr. N. RACHEGOWDA,*** *Professor, Department of Radiodiagnosis, Sri Devaraj Urs Medical College, Kolar, for his able guidance, constant encouragement, immense help and valuable advices which went a long way in moulding and enabling me to complete this work successfully. Without his initiative and constant encouragement this study would not have been possible. His vast experience, knowledge, able supervision and valuable advices have served as a constant source of inspiration during the entire course of my study. I would like to express my sincere thanks to* ***Dr.ANIL KUMAR SAKALECHA****., Professor and Head of Department of Radio-diagnosis, Sri Devaraj Urs Medical College for, valuable support, guidance and encouragement throughout the study. I would also like to thank* ***Dr. DEEPTI NAIK****, Professor, Department of Radio-diagnosis,* ***Dr. RAJESWARI*** *, Asst. prof, Department of Radio-diagnosis, and* ***Dr. RAVINDRA NAIK*** *, Asst. prof, Department of Radio-diagnosis, Sri Devaraj Urs Medical College for their wholehearted support and guidance.*

I would like to thank ***Dr. DARSHAN A.V, Dr. T. SAI SOUMYA, Dr. AMRUTHA, Dr. VINEELA****. and all my teachers of Department of Radio diagnosis, Sri Devaraj Urs Medical College and Research Institute, Kolar, for their constant guidance and encouragement during the study period.*

I am extremely grateful to the patients who volunteered for this study, without them this study would just be a dream.

I am thankful to my ***postgraduates DR.YASHAS ULLAS., DR.VARSHITHA G.R., DR. AASHISH., DR.CHAITANYA, DR. LYNN JOY, DR. KALATHURU UHA SAI, Dr. MAHIMA, Dr. ARUN RAJKUMAR, Dr. REVANTH R.B, Dr. PRAVEEN, Dr. NIKHILENDRA REDDY, Dr. MADAN and Dr. BUCCHIPUDI SANDEEP REDDY*** *for having rendered all their co-operation and help to me during my study.*

My sincere thanks to ***Mr. SUNIL, Mrs. NASEEBA*** *along with* ***KALMESH S (Sree Sai Enterprises)*** *and rest of the computer operators.*

I am also thankful to ***Mr. RAVI,*** *and* ***Mr. SUBRAMANI*** *with other* ***technicians*** *of Department of Radiodiagnosis, R.L Jalappa Hospital & Research Centre, Tamaka, Kolar for their help.*

I would also like to thank my friend ***Dr. MARIAM SHARIFF*** *for being constant support in all the tough times.*

Dr. MONISHA V.

Post graduate,

Department of Radio-diagnosis.

TABLE OF CONTENTS

LIST OF TABLES

LIST OF FIGURES

LIST OF ABBREVIATIONS

GLOSSARY	ABBREVIATIONS
ADC	Apparent diffusion coefficient
ANS	Autonomic nervous system
ATA	American thyroid association
AUS	Atypia of undetermined significance
CI	Confidence interval
CNS	Central nervous system
CT	Computed tomography
DTD	Diffuse thyroid disease
DWI	Diffusion-weighted imaging
ECA	External carotid artery
FLUS	Follicular lesion of unknown significance
FN/SFN	Follicular neoplasm/suspicious for follicular neoplasm
FNA	Fine-needle aspiration
FNAB	Fine-needle aspiration biopsy
FNAC	Fine needle aspiration cytology
FOV	Field of view
HPE	Histopathology
IQR	Quantitative values
MEN	Multiple endocrine neoplasia
MR	Magnetic resonance
MRI	Magnetic resonance imaging
MTCs	Medullary thyroid cancers
NMR	Nuclear magnetic resonance
NMTCs	Non-medullary thyroid cancers
PET	Positron emission tomography
RET	Rearranged during transfection
RF	Radio frequency

ROC	Receiver operating characteristic
SE	Spin-echo
SI	Signal intensity
TE	Time to Echo
TR	Repetition Time
TSH	Thyroid-stimulating hormone
US	Ultrasonography

ABSTRACT

Introduction: Thyroid nodules are most frequently noticed in clinical practice. Although the majority of these nodules are benign, up to 15% of them are malignant. Advanced diagnostic imaging tools, which are non-invasive such as DWI techniques, have been accurate in discriminating the growth of thyroid nodules. The aim of the present study was to assess the role of DWI and ADC in discriminating the growth (malignant and benign) and to determine other imaging features that can help in identifying neoplastic etiology.

Material and methods: This study was a cross-sectional study involving subjects with thyroid swelling or nodule on clinical examination and on ultrasonography. ADC values were computed for the different b-values. Histopathology results were obtained for all the patients. ADC values of benign and malignant thyroid lesions were compared with the histopathology results. *P*-value < 0.05 was considered as statistically significant.

Results: The sample size was 43 subjects, and female subjects were in the majority. The difference in the proportion of HPE findings between ADC values of the thyroid nodules was statistically significant (P-value <0.001). The ADC cut off value of 1.15 x 10^{-3} mm^2/s resulted in sensitivity of 87.50% in predicting final HPE diagnosis. Specificity was 94.29%, and the total diagnostic accuracy was 93.02%. The ADC value of thyroid nodules obtained had excellent predictive validity in predicting malignancy, as indicated by the area under the curve of 0.925 (P-value <0.001).

Conclusions: Using b factor of 800, ADC cut off value of 1.15 x 10^{-3} mm^2/s resulted in accuracy, sensitivity and specificity of 93.02 %, 87.50 %, and 94.29 %, respectively for discriminating between malignant and benign thyroid nodules.

Key words: thyroid nodule, MRI, ADC mapping, Diffusion weighted MRI.

INTRODUCTION

INTRODUCTION:

The most common pathology of the thyroid gland is thyroid nodules. Thyroid cancer has been on the rise in terms of incidence and prevalence. The prevalence of thyroid disorders is 0.8% out of all malignancies. The prevalence is significantly higher in females than males, and it was also higher in the age group >31 years. Thyroid illness incidence and prevalence have risen dramatically in recent years.[1] Thyroid cancer is becoming more common around the world, according to reports.[2] Over the last 30 years, the described prevalence of thyroid cancer has augmented to 0.07 percent.[3] Thyroid cancer was responsible for 344,670 new cases and 1,690 fatalities in 2010. According to statistics, thyroid cancer is growing more widespread around the world.

There are 2 types of thyroid disease: diffuse and nodular. Thyroid dysfunction is often related to Diffuse thyroid disease (DTD), and the thyroid function test and serology are commonly used to assess thyroid dysfunction. However, precise detection of subclinical or asymptomatic DTD in clinical practice is difficult. But it can aid in the proper therapy of thyroid dysfunction.[4]

Though fine-needle aspiration biopsy (FNAB) is considered the gold standard for diagnosis, it has been observed that FNAB results can be misleading in some cases.[5] Although ultrasound is the most frequent noninvasive and sensitive diagnostic imaging modality for identifying thyroid abnormalities, no acceptable criteria for distinguishing benign from malignant lesions exist. Furthermore, when the nodule is big or multinodular, accessing the malignancy of the tumour is challenging.[6]

Thyroid ultrasonography (US) is the frequent method used in identifying thyroid nodules.[7] Although clinical and laboratory results have played an important role in the diagnosis and treatment of DTD, thyroid ultrasound can be used to detect DTD.[8,9] Furthermore, recent research has shown that computed tomography (CT) can help detect DTD.[10,11]

Because CT is extensively used in the evaluation of neck lesions, it may be possible to diagnose DTD using it. Magnetic resonance imaging (MRI) has been shown in the literature to be useful in distinguishing Grave's illness from Hashimoto thyroiditis or painless thyroiditis.[12] On T1/T2-weighted images, Hashimoto thyroiditis, and Graves' disease show increased signal intensity (SI), whereas the normal thyroid shows slightly higher SI than nearby muscle on both scans. Diffusion-weighted MRI may also be useful in determining the difference between Hashimoto thyroiditis, Grave's disease, and painless thyroiditis.[12,13] However, no previous research has explored the possibility of using MRI to accidentally discover DTD.

Despite significant advancements in diagnostic techniques like ultrasonography, radionuclide imaging, and CT, finding a non-invasive and reliable method to distinguish benign from malignant lesions remains a major challenge. Some MR protocols may have diagnostic utility for various types of lesions, according to recent advances in MRI. Thyroid lesions can be identified and measured using routine T1 and T2 weighted MR imaging. However, these techniques lack the specificity needed to identify benign from malignant thyroid nodules or to assess the functional status of these nodules.[14]

"Diffusion-weighted MR imaging" (DWI) is a new approach for detecting illnesses of the central nervous system (CNS). DWI is sensitive to changes in tissue microstructure that could

alter water diffusion. It's been used to assess head and neck tumours in a variety of ways. [15,16] The Apparent Diffusion Coefficient (ADC) value is a statistical value derived from DWI scans which could be used to differentiate malignant from benign lesions.

NEED FOR THE STUDY:

With 42% frequency in ultrasound examination, thyroid nodules play a big challenge for both radiologists and clinicians. Most of these nodules are benign; however, up to 7% will turn out to be malignant, requiring proper management.[17] According to American Thyroid Association guidelines, ultrasound is the imaging modality of choice for assessment and risk stratification of thyroid nodules.[18] Various sonographic features are used for the characterization of thyroid nodules and for deciding if fine-needle aspiration (FNA) is required or not. For further evaluation of suspicious nodules, FNA is considered the diagnostic method of choice. FNA is an invasive procedure and highly inaccurate in nodules larger than 4 cm.[19]

Thyroid nodules are frequently discovered in computed tomography or magnetic resonance imaging (MRI); however, these modalities are not reliable for the characterization of thyroid nodules.[20] Ultrasound is usually indicated in these incidentally detected nodules. Various studies have assessed the power of diffusion-weighted imaging (DWI) and its quantitative counterpart apparent diffusion correction (ADC) for differentiation between benign and malignant thyroid nodules. The results of these studies have been promising, but wide variability has been encountered.[2,21,22]

Earlier, DW-MRI was mainly used for the detection of cerebral ischemia in the brain, but over the last two decades it is being used in other extracranial lesions.[23,24] Cancer is characterized by increased cellularity and hence shows restricted diffusion of water molecules. It has been seen that ADC is related to the cellular density of the tumors.[23–25] Most

of the malignant tumors show reduced ADC due to high cellularity and reduced extravascular extracellular space.[24] Hence, ADC values calculation can distinguish malignant from benign thyroid nodules.[25] There is a scarcity of literature in this field pertaining to the Indian context.[26] Hence this study was designed to assess the accuracy of DWI MRI for distinction between benign and malignant thyroid nodules using a 1.5-T MRI.

AIMS & OBJECTIVES

AIM AND OBJCETIVES:

1. To evaluate the morphology of thyroid nodules on MRI.
2. To correlate DWI-MRI findings with pathological findings
3. To determine an apparent diffusion coefficient cutoff value to differentiate benign from malignant nodules using DWI.

Research question

Can DWI with ADC help in differentiating benign from malignant thyroid nodules accurately?

REVIEW OF LITERATURE

REVIEW OF LITERATURE:

1. Thyroid nodules

The thyroid nodule is defined by the American Thyroid Association (ATA) as a distinct lesion within the thyroid gland. It is radiographically different from the thyroid parenchyma around it. [18] Solitary, numerous cystic, or solid nodules are all possible.[27]

Thyroid nodules are a common occurrence, with physical examination alone detecting them in around 5% to 7% of the adult population. Autopsy data, on the other hand, revealed a 50% frequency of thyroid nodules larger than one centimeter in patients who had never been diagnosed with thyroid illness. Due to the widespread use of contemporary imaging modalities, such as ultrasound (US), computed tomography (CT), MRI, and positron emission tomography (PET), nodules are becoming more common.[28]

Thyroid nodules are vital because they may indicate thyroid malignancy in about 4.0 percent to 6.5 percent of cases, despite the fact that > 90% of identified nodules are clinically unimportant benign lesions.[29]

Anatomy of the thyroid gland:

The thyroid gland is a midline structure located in the anterior neck. The thyroid functions as an endocrine gland and is responsible for producing thyroid hormone and calcitonin, thus contributing to the regulation of metabolism, growth, and serum concentrations of electrolytes such as calcium.[27]

The thyroid gland is grouped into 2 lobes that are connected by the isthmus, which crosses the midline of the upper trachea at the second and third tracheal rings. In its anatomic position,

the thyroid gland lies posterior to the sternothyroid and sternohyoid muscles, wrapping around the cricoid cartilage and tracheal rings. It is located inferior to the laryngeal thyroid cartilage, typically corresponding to the vertebral levels C5-T1. The thyroid attaches to the trachea via consolidation of connective tissue, referred to as the lateral suspensory ligament or Berry's ligament. This ligament connects each of the thyroid lobes to the trachea. The thyroid gland, along with the esophagus, pharynx, and trachea, is found within the visceral compartment of the neck, which is bound by pretracheal fascia.

The "normal" thyroid gland has lateral lobes that are symmetrical with a well-marked centrally located isthmus. The thyroid gland typically contains a pyramidal extension on the posterior-most aspect of each lobe, referred to as the tubercle of Zuckerkandl. Despite these general characteristics, the thyroid gland is known to have many morphologic variations. The position of the thyroid gland and its close relationship with various structures brings about several surgical considerations with clinical relevance.

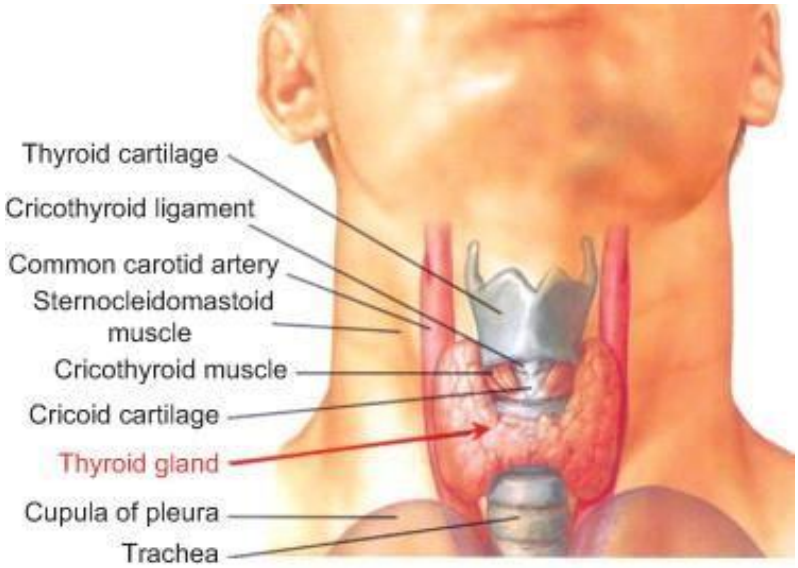

Figure 1: Gross anatomy of the thyroid gland.[30]

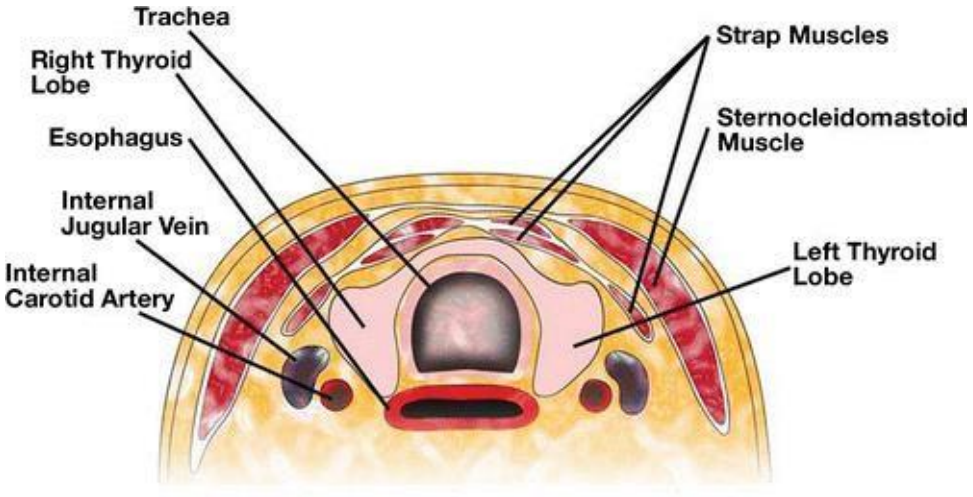

Figure 2: Drawing illustrates thyroid and adjacent soft-tissue structures anatomy in cross-sectional view.[20]

Embryology:

The parenchyma of the thyroid gland is derived from the endoderm. The thyroid gland originates from the foramen cecum, which is a pit positioned at the posterior one-third of the tongue. Early in gestation, the thyroid gland begins its descent anterior to the pharynx as a bilobed diverticulum. The thyroid gland then continues to descend anterior of the hyoid bone and the cartilages of the larynx. By the seventh week, the thyroid gland reaches its destination midline and anterior to the upper trachea. The thyroglossal duct maintains the connection of the thyroid gland to the base of the tongue until involution and disappearance of the duct.

The ultimobranchial body, derived from the ventral part of the fourth pharyngeal pouch, then becomes incorporated into the dorsal aspect of the thyroid gland. The ultimobranchial body gives rise to the parafollicular cells or C cells of the thyroid gland.

Blood Supply and Lymphatics:

The thyroid gland has an extremely rich blood supply and is estimated to be six times as vascular as the kidney and relatively three to four times more vascular than the brain. It receives blood from the superior and inferior thyroid arteries. The superior and inferior aspects of the gland are supplied by these paired vessels. The superior thyroid artery, which begins near the level of the superior horn of the thyroid cartilage, is the 1st branch (ECA). The superior thyroid artery then moves anterior, inferior, and towards the midline behind the sternothyroid muscle to the superior pole of the lobe of the thyroid gland. From this point, the superior thyroid artery branches off. One branching point runs down the dorsal aspect of the thyroid gland. The other superficial branch runs along with the sternothyroid muscle and thyrohyoid muscles, supplying branches to these muscles as well as the sternohyoid. The superficial branch continues downward to further give off the cricothyroid branch and to supply the isthmus, inner sides of the lateral lobes, and when present, the pyramidal lobe.[31]

The thyrocervical trunk arises from the anterosuperior surface of the subclavian artery and gives rise to three branches, one being the inferior thyroid artery. The inferior thyroid artery branches from the thyrocervical trunk at the inner border of the anterior scalene muscle and advances medially to the thyroid gland. The artery reaches the posterior surface of the lateral lobe of the thyroid gland at the level of the junction of the upper two-thirds and lower third of the outer border. The largest branch of the inferior thyroid artery is the ascending cervical branch, and it is important not to mistake this branch for the inferior thyroid artery itself.[32]

In 10% of the population, there is an additional artery known as the thyroid ima artery. This artery has a variable origin, including the brachiocephalic trunk, aortic arch, the right common carotid, the subclavian, the pericardiacophrenic artery, the thyrocervical trunk, transverse

scapular, or internal thoracic artery. The thyroid ima most commonly originates from the brachiocephalic trunk and supplies the isthmus and anterior thyroid gland.[32]

The thyroid gland is drained via the superior, middle, and inferior thyroid veins. The middle and superior thyroid veins follow a tortuous route and eventually drain into the internal jugular vein on either side of the neck. The drainage of the inferior thyroid vein may enter either the subclavian or brachiocephalic veins, located just posterior to the manubrium.

Lymphatic drainage of the thyroid gland involves the lower deep cervical, prelaryngeal, pretracheal, and paratracheal nodes. The paratracheal and lower deep cervical nodes, specifically, receive lymphatic drainage from the isthmus and the inferior lateral lobes. The superior portions of the thyroid gland drain into the superior paratracheal and cervical nodes.

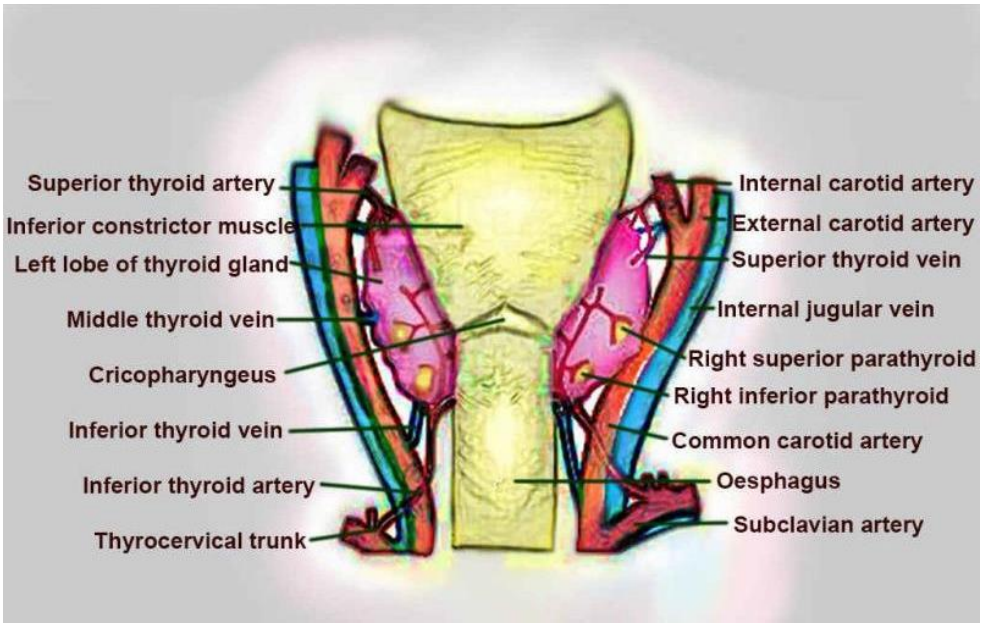

Figure 3: Showing the arterial and venous supply to thyroid gland.[31]

Nerves:[33]

The ANS ("autonomic nervous system") primarily innervates the thyroid gland. The vagus nerve provides the main parasympathetic fibers, while sympathetic fibers originate from the inferior, middle and superior ganglia of the sympathetic trunk. These nerves do not play a role in the control of hormonal production or secretion but mostly influence vasculature.[32]

Muscles:[33]

Several muscles should be considered when discussing neck and thyroid surgical anatomy.

- Platysma: The first muscle encountered during neck dissection; it is enveloped by the superficial cervical fascia. It sits in the anterior neck and extends from the superficial fascia of the deltoid over the clavicle, reaching the mandible and superficial fascia of the face superiorly.
- Sternocleidomastoid: This muscle forms the anterior portion of the posterior triangle of the neck. The muscle runs obliquely from the mastoid to the clavicle and sternum. The sternocleidomastoid is found anterolaterally relative to the thyroid gland.
- Digastric muscle: This muscle extends from the mandibular tubercle, passes deep and inferior to the hyoid, and loops back up to attach to the mastoid tip.
- Infrahyoid muscles: These are also referred to as "strap muscles." They include four paired muscles found on the anterolateral surface of the thyroid gland. The strap muscles result in gross movement of the larynx during swallowing and also adjust the positioning of the larynx during vocalization.
- Omohyoid muscle: The omohyoid muscle is found deep to the sternocleidomastoid. It extends from the hyoid bone to the lateral aspect of the clavicle.

- Sternohyoid muscle: This muscle sits anterior to the remaining strap muscles and the thyroid gland. The sternohyoid muscle extends from its superior attachment at the hyoid bone inferiorly to the sternum.
- Sternothyroid muscle: This muscle extends from the oblique line of the thyroid cartilage to the sternum. This muscle contacts the anterior surface of the thyroid gland.
- Thyrohyoid muscle: The thyrohyoid muscle extends from the oblique line of the thyroid cartilage to the hyoid bone superiorly.
- Inferior pharyngeal constrictor: This muscle extends from its anterior attachment at the oblique line of the thyroid cartilage and lateral aspect of the cricoid cartilage to the pharyngeal raphe. This muscle contacts the superior pole of the lateral lobe of the thyroid gland medially.

Etiology:

Thyroid nodules can be caused by a variety of illnesses, ranging from benign to malignant ailments with indolent to aggressive clinical histories. Within a multinodular goitre, about 23% of solitary nodules constitute a dominant nodule.[34]

Ionizing radiation is a known risk factor for thyroid nodules, both benign and malignant. Thyroid nodules may form at a rate of 2% each year in this group. In palpable nodules of previously irradiated thyroid glands, the incidence of cancer has been reported to be as high as 20% to 50%.[35]

Smoking, obesity, metabolic syndrome, alcohol intake, elevated levels of insulin-like growth factor-1, and uterine fibroids are all risk factors for thyroid nodules and goitre. Oral contraceptives and statins are two factors that have been linked to a reduced risk.[36]

There are two types of thyroid nodules: neoplastic and non-neoplastic. Neoplastic nodules can be benign or malignant, and benign neoplastic nodules can be both non-functional and functioning. Hyperplastic and inflammatory nodules are examples of non-neoplastic nodules.[27]

Colloid nodules, which are the most frequent thyroid nodules, are adenomatous benign neoplasms with no elevated risk of cancer. While most follicular adenomas are benign, they are similar to follicular carcinomas in appearance.[35]

Thyroid carcinomas are divided into two types: non-medullary thyroid cancers (NMTCs), which arise from epithelial cells and account for around 95% of all thyroid cancers, and medullary thyroid cancers (MTCs), which arise from the thyroid's calcitonin-producing parafollicular cells. Twenty percent of MTCs are well-known, and they can arise as part of MEN (multiple endocrine neoplasia) syndromes [36]

Epidemiology:

The frequency of a disease is determined by the screening method used, and the population studied. With increasing age, feminine gender, iron insufficiency, and thyroid radiation history, the chance of thyroid nodules increases.[37] Long-term survivors of hematopoietic stem cell transplantation have a relative risk of 3.26 for subsequent thyroid cancer.[38]

Physical examination alone reveals the frequency of thyroid nodules in the younger population of 5% to 7%. In this same cohort, ultrasound reveals a prevalence of 20% to 76%, which corresponds to autopsy findings.[29]

Thyroid nodules are four times more common in females than in males, and they are more common in people who live in iodine-deficient areas.[35] According to 20-year surveillance research, men and women have a prevalence of 0.8 percent and 5.3 percent, respectively.[39] Men, on the other hand, have double the cancer rate as women (8 percent versus 4 percent).[40]

Pathophysiology:

The pathophysiology of a thyroid nodule varies according on the type of lesion. Thyroid nodules can be caused by a variety of conditions. Benign macrofollicular nodules, which can be monoclonal adenomas or colloid nodules in a multinodular goitre, are the most prevalent kind. The latter refers to the growth of monoclonal cells that replicate in a nodular form. Follicular neoplasms may pose a diagnostic challenge because they are similar to all other carcinomas.[41]

There is a well-established link between thyroid irradiation and cancer. Radiation can generate a variety of somatic mutations that increase cancer risk, especially in radiation-sensitive tissues like the thyroid. Children have a higher risk of thyroid cancer after irradiation than adults; this is most likely due to the thyroid tissue's higher proliferative activity in younger people. In thyroid cancers linked to ionizing irradiation RET proto-oncogene translocations have been discovered.[29,42]

Histopathology:

The 2 most commonly used diagnostic techniques for assessing cytopathology of thyroid nodules are FNA and fine-needle capillary sampling (FNC). The National Cancer Institute recommends using the Bethesda classification that stratifies cytologic findings into 6 major categories, each showing different subsequent evaluation and management.[43]

The Bethesda system diagnostic categories for reporting thyroid cytopathology describes:[18,44]

1. Non-diagnostic: Represents an inadequate sample with an insufficient number of follicular cells

2. Benign, normal thyroid tissue, showing nodules of adenomatous or multinodular goiters, common entities include adenomatous nodules, Hashimoto thyroiditis, and subacute granulomatous thyroiditis.

3. Follicular lesion of undetermined significance (FLUS) or atypia of undetermined significance (AUS): proposed for lesions that are not convincingly benign.

4. Follicular neoplasm or suspicion for follicular neoplasm includes microfollicular or cellular adenomas.

5. Suspicious for malignancy: Includes lesions with features of malignancy that are not definitive for thyroid cancer.

6. Malignancy: Cytology will differ on the different types of possible thyroid malignancies.

History and Physical examination:

The majority of patients will have a big palpable lump in the anterior neck, or an incidental nodule will be discovered on imaging examinations done for other reasons. The majority of thyroid nodules are asymptomatic, and the majority of people with nodules are euthyroid, with only about 1% of nodules causing thyroid illness. Some individuals may experience neck pressure or pain, especially if they have a spontaneous haemorrhage.[35]

With a prevalence of 4 percent to 7 percent, thyroid palpation is the simplest but least sensitive approach for finding thyroid nodules. Nodules bigger than 4 cm in diameter (about 19 percent risk for malignancy), stiffness on palpation, fixation to neighbouring tissues, cervical lymphadenopathy, and vocal fold paralysis are all physical examination symptoms that should raise concern for malignancy. The physical examination of some patients may be limited by their body habitus.[28]

The physical examination findings of a solitary nodule, as well as cervical lymphadenopathy (more than 1 cm) and vocal fold paralysis, have a positive predictive value of 100 percent for thyroid cancer.

A complete social history is essential for identifying patients with MEN II syndrome. These people are more likely to develop pheochromocytomas and require a thorough examination before undergoing surgery.[36]

Evaluation:

History, physical examination, thyroid-stimulating hormone (TSH) measurement, and thyroid ultrasonography to describe the nodule should all be part of the initial evaluation for individuals with thyroid nodules. TSH measurement may be able to detect minor thyroid dysfunction on its own.[45]

Serum markers, fine-needle aspiration (FNA) cytology, genetic markers, immunohistochemical markers, and numerous imaging modalities, including ultrasonography, elastography, MRI, CT, and 18 FDG-PET scans, are all part of the diagnostic workup.[36]

Thyroid-stimulating hormone (TSH) measurement should be the first test and used as a reference for future care in any patient with a thyroid nodule. A normal or high TSH can be concerning because the risk of cancer rises in lockstep with the level of serum TSH. A low TSH, on the other hand, usually indicates a benign nodule. In a patient with low TSH, an iodine-123 or pertechnetate scintigraphy scan is used to assess the probability of an autonomously functioning thyroid nodule. Thyroid nodules that function independently are almost always benign and require no additional testing.[38]

Thyroid ultrasonography (US) is an important imaging technique for evaluating thyroid nodules. It can detect lesions as tiny as 2 mm and offer information on their size, structure, andparenchymal alterations. It is widely utilized to distinguish between benign and malignant lesions in order to prevent intrusive operations that aren't essential. Several characteristics have been linked to cancer and identified as independent risk factors. Microcalcifications, uneven edges, hypoechogenicity, a taller-than-wide form, and enhanced vascularity are only a few of them.[36]

Thyroid nodules that are too tiny to palpate can be detected with great sensitivity using the US. However, the clinical relevance of these nodules is unknown. In individuals who had previously been diagnosed with primary non-thyroid cancer, incidental thyroid nodules had a malignancy risk of 24%. This is far higher than the estimated 5 % point malignancy rate in patients with no additional primary tumour.[38]

FNA is the most cost-effective diagnostic method utilized in the assessment of thyroid nodules, and it is used in conjunction with the US. Palpation-guided biopsies are associated with a higher proportion of false-negative findings and non-diagnostic cytology; hence its usage under US guidance is preferred.

The choice to do FNA should be based on an individual risk assessment based on the patient's medical history, clinical findings, and ultrasound findings. When there is more than one worrisome US characteristic, cervical lymphadenopathy, or a high-risk history, even nodules smaller than one centimeter are biopsied. For solid nodules with only one worrisome US characteristic, a cutoff size of one centimeter is employed.[34]

In individuals with the following conditions, a US-FNA is recommended: [27]

- Nonpalpable thyroid nodules greater than 1 cm.
- Palpable thyroid nodules smaller than 1.5 cm.
- Deeply located nodules.
- Nodules close to blood vessels.
- Nodules following non-diagnostic conventional FNA cytology.
- Cystic or mixed nodules, especially if a previous conventional FNA was non-diagnostic.

- Lesions that are cystic or spongiform are thought to have a low risk of cancer and are monitored or biopsied if they are greater than 2 centimetres.[34]

Treatment / Management:

Thyroid nodule treatment is determined by the type of lesion discovered, its US features, and whether it is functional or not. The results of the FNA will eventually guide treatment.[27]

The results of FNA cytology are divided into six primary diagnostic groups (Bethesda classification), each of which indicates a particular course of treatment.[43]

1. Non-diagnostic: Cancer risk ranges from 5% to 10%.
2. Benign: Cancer risk ranges from 0% to 3%.
3. Uncertain significance atypia or undetermined significance follicular lesion: Cancer risk 10% to 30%
4. Follicular neoplasm (or suspicion of follicular neoplasm): Cancer risk ranges from 25% to 40%.
5. Suspicious of malignancy: Cancer risk ranges from 50% to 75%.
6. Carcinogenic: Cancer risk ranges from 97 to 99 percent.

Biopsies taken for non-diagnostic purposes (Bethesda I) are cytologically insufficient. If only a small amount of follicular tissue is retrieved, the absence of malignant cells should not be construed as a negative biopsy. In most cases, FNA is repeated within 4 to 6 weeks.[46]

Subjects with benign nodules (Bethesda II), such as macrofollicular, colloid, and nodular adenomas, nodular goitre, and Hashimoto thyroiditis, are routinely monitored without surgery. The use of periodic US monitoring, starting at 12 to 24 months and increasing in

intervals is recommended. Despite a benign initial biopsy, if the US reveals very worrisome results, FNA should be repeated within 12 months.[29]

The method varies with institutional practices for nodules with "atypia of undetermined significance" (AUS) and "follicular lesion of undetermined significance" (FLUS), while Bethesda category IV reflects "follicular neoplasm/suspicious for follicular neoplasm" (FN/SFN) (Bethesda III and IV). Some institutions collect a second FNA sample for genetic testing, while others repeat the FNA 6 to 12 weeks later. If recurrent aspirates reveal merely architectural atypia, a radionuclide scan may be ordered.[47]

Differential Diagnosis:

While the majority of nodules and masses in the anterior neck are benign thyroid nodules or cysts, malignancy should be ruled out, especially in patients who are at risk for thyroid cancer.[48]

The anterior neck may have congenital neck masses. These are most commonly present at birth, but others may appear later in life. The fact that the patient is older at the time of presentation should raise suspicion of cancer. Tongue cancer, tonsil cancer, and thyroid cancer can all show as cystic neck tumours. Inflammatory neck masses are frequently swollen lymph nodes that are caused by a viral or bacterial infection. These are frequently seen anterior to the trapezius muscle and superficial/deep/posterior to the sternocleidomastoid muscle. Metastatic neck masses are most usually associated with squamous cell carcinoma of the aerodigestive tract and other non-thyroid neoplastic illnesses.[48]

Prognosis:

The majority of thyroid nodules are harmless. Initial observations such as a normal to high serum TSH level, a history of irradiation or MEN, and various ultrasonographic characteristics such as hypoechogenicity, vascularity, taller-than-wide form, microcalcifications and uneven borders raise concerns for malignancy.[34] While solitary nodules have a higher risk of cancer than nodules within a multinodular thyroid, the overall risk of malignancy in a subject with a multinodular gland is about equal due to the additive risk of each lesion.[28]

Thyroid cancer prognosis varies widely based on the histological type and subtype of cancer, as well as various individual factors such as age at diagnosis, original tumour size, presence of soft tissue invasion, and distant metastasis.[49]

The majority of patients with papillary thyroid carcinoma do not die from it. Malignancy-related mortality was found to be 6% in one case series of patients with non-metastatic papillary thyroid carcinoma.[50]

Male gender, mediastinal lymph node involvement, delay in primary surgical therapy of more than 1 year following diagnosis of a nodule, and multicentricity of the intrathyroidal tumour are all related with an increased risk of malignancy recurrence or mortality.[50]

Follicular cancer is more common in elderly people and has a more aggressive course. It is frequently linked to distant metastases and a greater fatality rate than papillary thyroid cancer.[29]

Complications:

Patients with functioning thyroid nodules may experience hyperthyroidism symptoms as a side effect. Hyperthyroidism's clinical symptoms, such as sweating, palpitations, and reduced glucose tolerance will be present. The majority of thyroid nodules, on the other hand, are benign, and most patients will have no symptoms. Thyroid pain may be present in a small percentage of individuals, particularly those with cystic thyroid lesions, and may signal a sudden hemorrhage or hemorrhagic infarction.[29]

2. Role of MRI in the diagnosis of thyroid nodules

History:

The nuclear magnetic resonance (NMR) phenomenon was first described experimentally by both Bloch and Purcell in 1946, for which they were both awarded the Nobel Prize for Physics in 1952. The technique has rapidly evolved since then, following the introduction of wide-bore superconducting magnets (approximately 30 years ago), allowing the development of clinical applications. The first clinical magnetic resonance images were produced in Nottingham and Aberdeen in 1980, and magnetic resonance imaging (MRI) is now a widely available powerful clinical tool.[51]

Principle: MRI is a non-invasive method of mapping the internal structure and certain aspects of function within the body. It uses nonionizing electromagnetic radiation and appears to be without exposure-related hazards. It employs radio frequency (RF) radiation in the presence of carefully controlled magnetic fields in order to produce high-quality cross-sectional images of the body in any plane. The MR image is constructed by placing the patient inside a large magnet which induces a relatively strong external magnetic field. This causes the nuclei of many atoms in the body including hydrogen to align with the magnetic field and later on application of RF signal energy is released from the body, detected, and used to construct the MR image by Computer.[52]

The steps involved in the production of an MRI study may be summarized as follows:[52]

1. A powerful, uniform external magnetic field is employed to align the normally randomly oriented water contained in the tissue being examined.
2. This alignment (or magnetization) is next perturbed or disrupted by the introduction of external RF energy at an appropriate frequency so as to induce resonance. Spatial localization is obtained through the application of a spatially dependent magnetic field (referred to as a gradient) during the same time that RF energy is introduced into the tissue. The gradient field selectively modulates the resonant frequency of the patient in accordance to the Larmor equation.
3. The nuclei return to their restive alignment through various relaxation processes and, in so doing, emit RF energy proportional to the magnitude of their initial alignment or magnetization.
4. After an appropriate period following initial RF deposition, the emitted signals are measured or read out.
5. A mathematical process called Fourier transformation is used to convert the frequency formation contained in the signal from each location in the imaged plane to corresponding intensity levels, which are then displayed as shades of gray in a matrix arrangement of, for example, 256 X 256 pixels.
6. Protons in the various tissues in the imaged slice realign with the magnetic field at different rates so that at any given moment, there is a difference in signal strength between various tissues. This difference in signal strength from region to region constitutes the basis of tissue contrast and forms the substrate for interpretation of the image.

Morphology of thyroid nodule on MRI:

- The thyroid glands MRI features are as follows:
- On T1/T2-weighted images, the typical thyroid parenchyma has an iso-/slightly high SI.
- SI was homogenous in all normal thyroid parenchyma cases, the anteroposterior diameter of the thyroid gland was normal, the thyroid gland had a smooth edge, and the enhancement was homogeneously raised when compared to the surrounding muscle.[14]

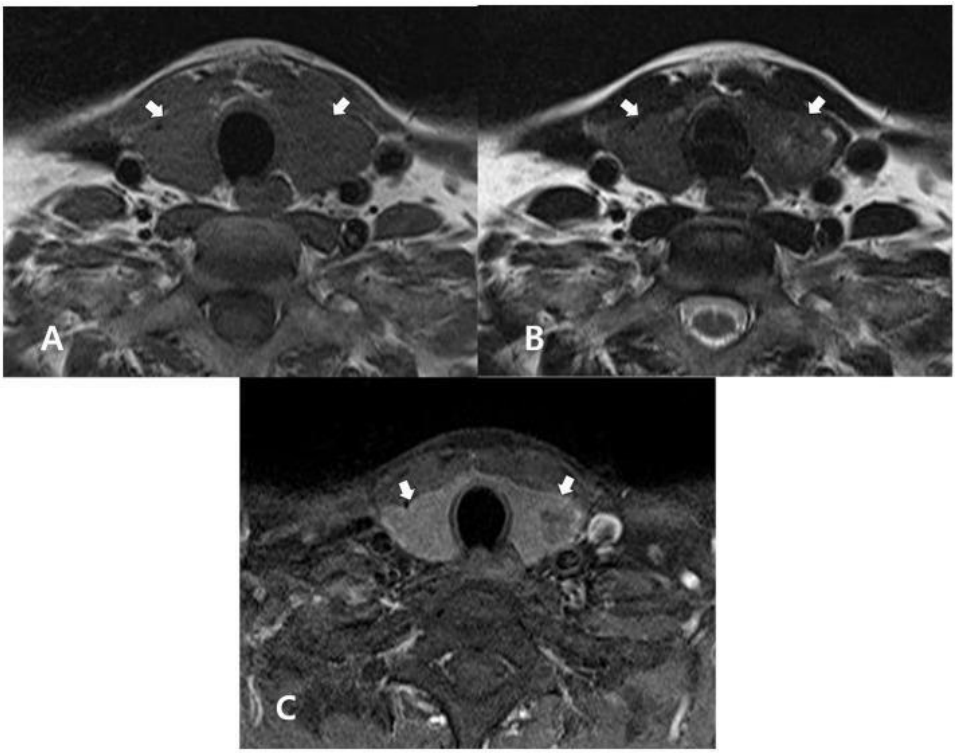

Figure 4: On MRI, normal thyroid parenchyma can be visible. When compared to nearby muscle, the thyroid gland (arrows) exhibits homogenous, isointense and somewhat elevated signal intensities in non-enhanced axial T1(A) and T2(B) weighted images. The thyroid gland (arrows) is typical in size and has a smooth border in both the images. When compared to nearby muscle in the enhanced axial, fat-suppression T1-weighted picture (C), the thyroid gland (arrows) demonstrates homogeneously greater enhancement.[14]

3. Role of Diffusion-Weighted MRI in differentiating benign from malignant nodules.

Since the 1990s, diffusion-weighted imaging has been utilized to diagnose early stroke and other neurologic disorders. Since then, a rising number of studies have proved the method's utility in the diagnosis and characterization of lesions, particularly in the field of oncologic imaging. With new technical developments in magnetic resonance (MR) imaging, such as multichannel coils, echoplanar imaging, and stronger gradients, the use of a diffusion-weighted sequence in whole-body imaging has grown in popularity, resulting in a reduction in the amount of time required for diffusion-weighted imaging to less than 1 minute.[53] As a result, these sequences can be added to the imaging routine without raising the overall acquisition time much. Another advantage of diffusion-weighted imaging is that it uses intrinsic tissue contrast rather than external contrast material. Diffusion-weighted imaging is increasingly being used for specialized purposes as a result of the aforementioned advancements and a growing amount of research.[54]

Diffusion-weighted Imaging Technique:

The most popular method for diffusion-weighted imaging is to combine two symmetric motion-probing gradient pulses, one on either side of the 180° refocusing pulse, into a single-shot spin-echo (SE) T2-weighted sequence (Stejskal-Tanner sequence). This is due to the fact that a diffusion gradient causes the phase shift to vary with position, with any spins that remain in the same place (i.e., confined diffusion microenvironment) along the gradient axis during the two pulses returning to their initial state. However, spins that have migrated (i.e., free water molecules) will be exposed to a different field strength during the second pulse and will not revert to their initial state but will instead undergo a total phase shift, resulting in a drop in the recorded MR signal intensity. The degree of signal attenuation is determined by a number of parameters, as illustrated in the equation below:[55]

$$SI = SI_0 \times \exp(-b \times D),$$

"SI0 is the signal intensity of a T2-weighted image without a diffusion gradient, b is the degree of diffusion weighting (b value), and D is the diffusion coefficient".[54]

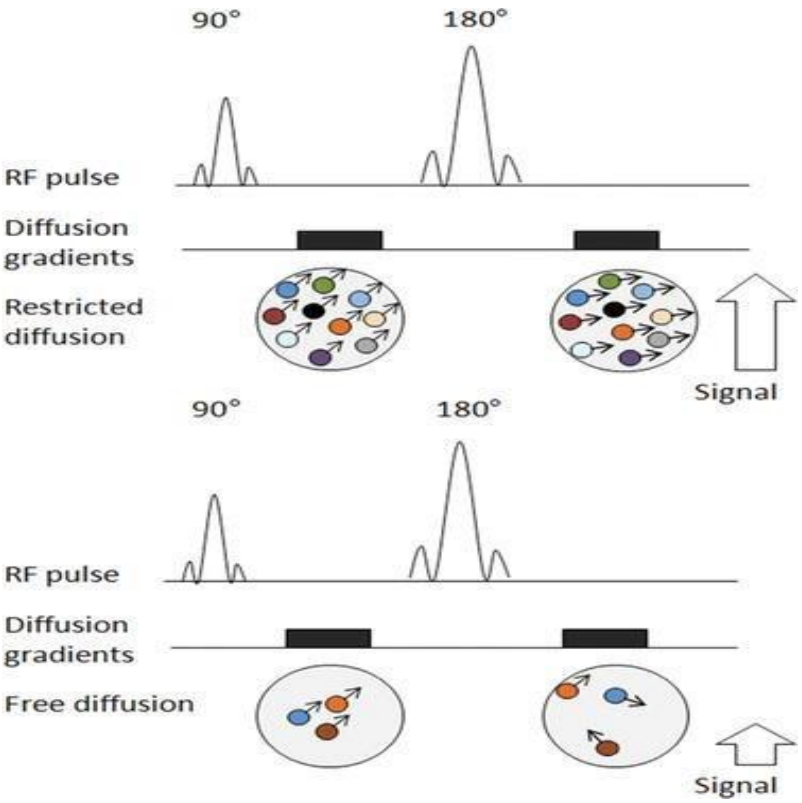

Figure 5: Pulse sequence diagrams illustrate how a diffusion-weighted sequence incorporates two symmetric motion-probing gradient pulses into a single-shot SE T2 weighted sequence, one on either side of the 180° refocusing pulse. Restricted diffusion (top) manifests as a retained signal, whereas free diffusion (bottom) translates into a signal loss. Increase the amplitude, duration, and temporal spacing of the two motion- probing gradients to increase the sensitivity of diffusion-weighted imaging to diffusion. *RF* = radiofrequency. Increase the amplitude, duration, and temporal spacing of the two motion-probing gradients to increase the sensitivity of diffusion-weighted imaging to diffusion. The b value (expressed in seconds per square millimeter), an index of the degree of diffusion weighting, is determined by these gradient parameters.

In clinical practice, multiple b values are used to reduce the error in ADC calculation for

improved characterization of tissue.[56]

Apparent diffusion coefficient (ADC) and its role in determining malignancy:

During post processing, the ADC is determined using at least two separate b values. The slope of the line superimposed on the plot of the logarithm of relative signal intensity (y-axis) versus b value is the ADC value (x-axis). Using more diffusion-weighted pictures with varied b values yields a more accurate ADC value. An ADC map is the final image with various ADC values generated for each pixel of an image. The ADC value for a lesion can be determined by sketching regions of interest within the lesion. Lower ADC values are seen in locations with more restricted diffusion and, as a result, higher diffusion-weighted signals. ADC maps exhibit inadequate anatomic detail and should be examined in conjunction with other MR images, such as different b-value diffusion-weighted images, higher-resolution anatomic pictures, and contrast material–enhanced images, if available.[56]

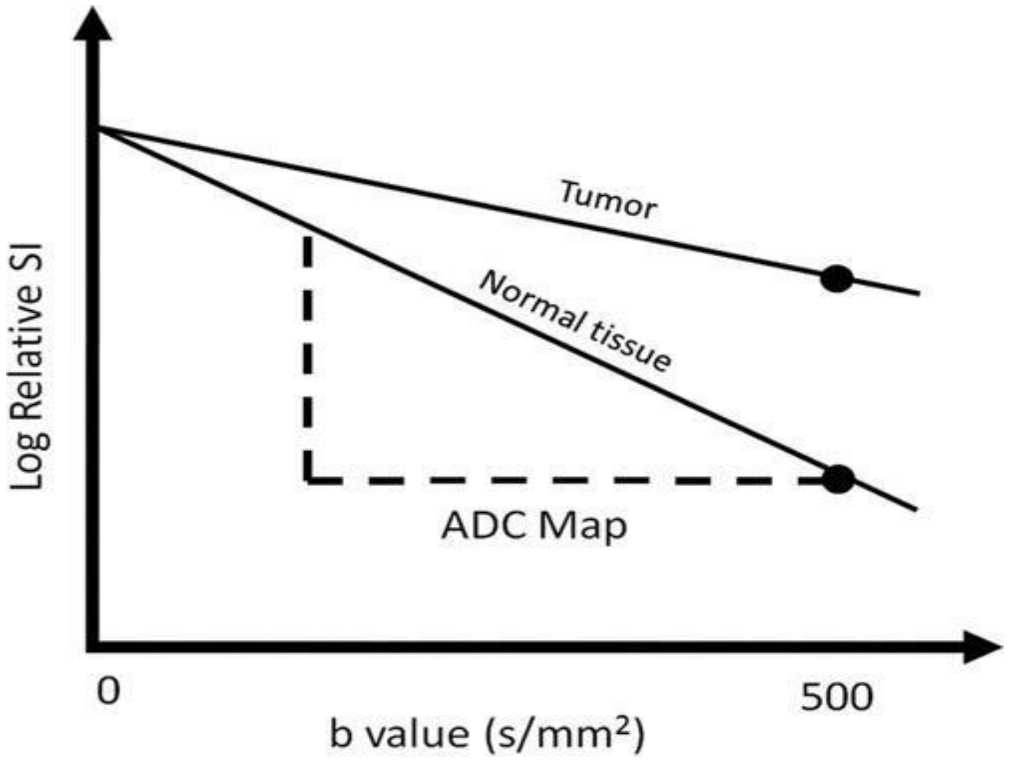

Figure 6: For tumor and normal tissue, the graph shows the logarithm of relative signal intensity (SI) (y-axis) versus b value (in this case, 0 and 500 sec/mm2) (x-axis). The slope of

the "tumor line" is lower than that of the "normal tissue line," resulting in less signal on the ADC map.[56]

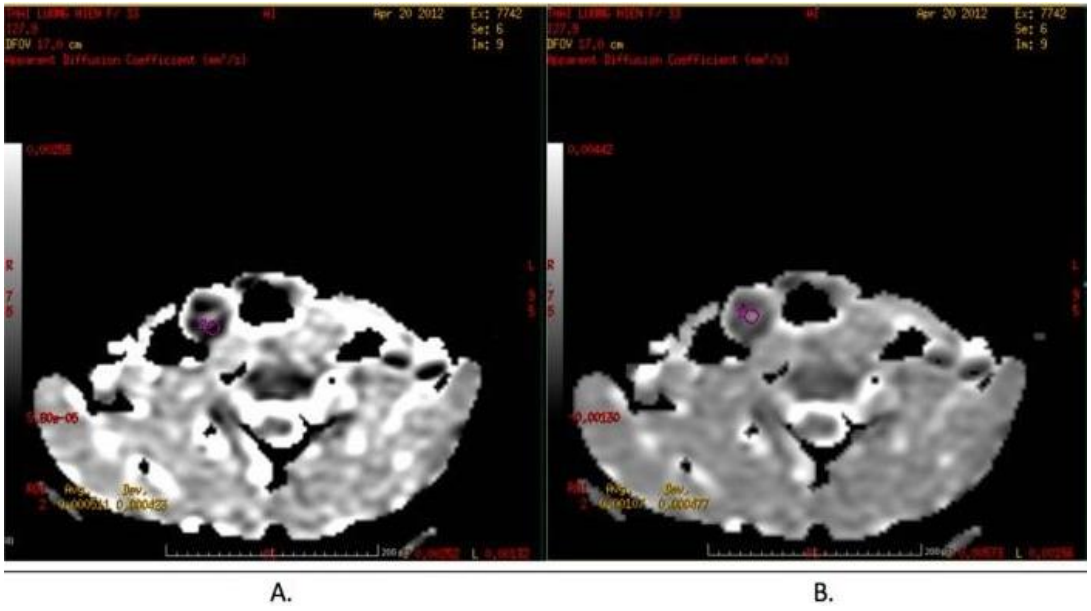

Figure 7: Demonstration on measuring ADC values accurately: (A) Right method. (B) Wrong method.[57]

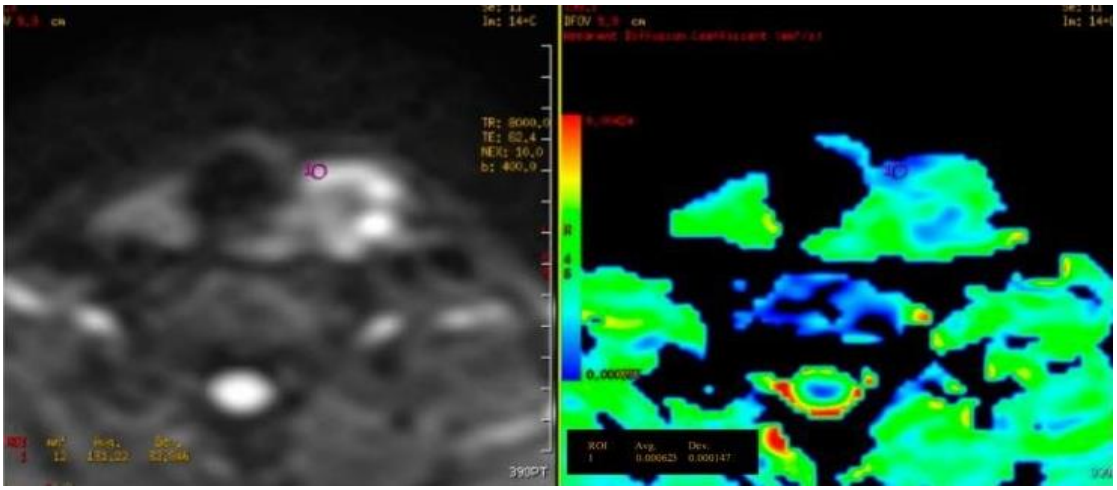

Figure 8: Mean ADC value of a malignant thyroid nodule with b = 800 was 0.62 $\times 10^{-3}$ mm^2/s. Histopathology result: Papillary carcinoma.[57]

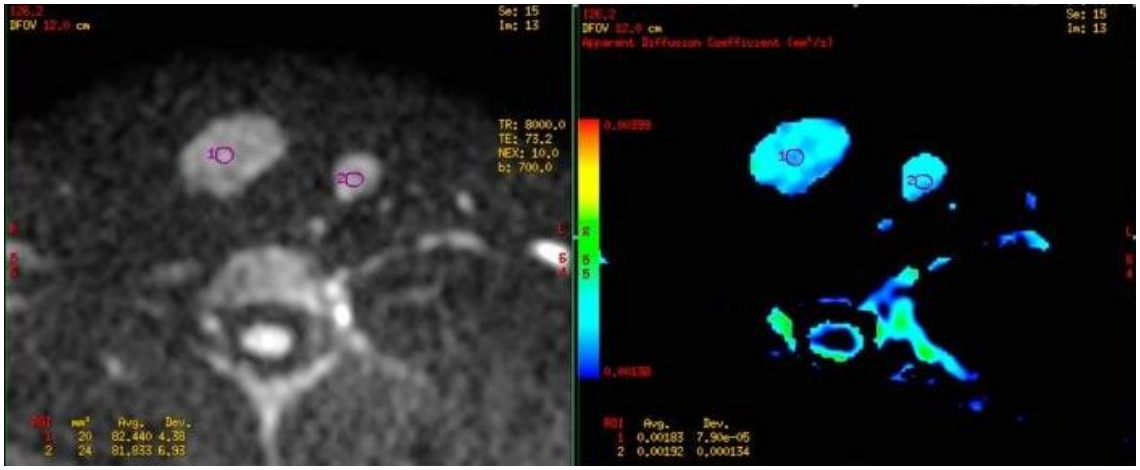

Figure 9: Right and left lobe thyroid nodules, with b = 700, ADC: 1.83 × 10^{-3} mm^2/s and 1.92 × 10^{-3} mm^2/s. Histopathology result: benign nodules.[57]

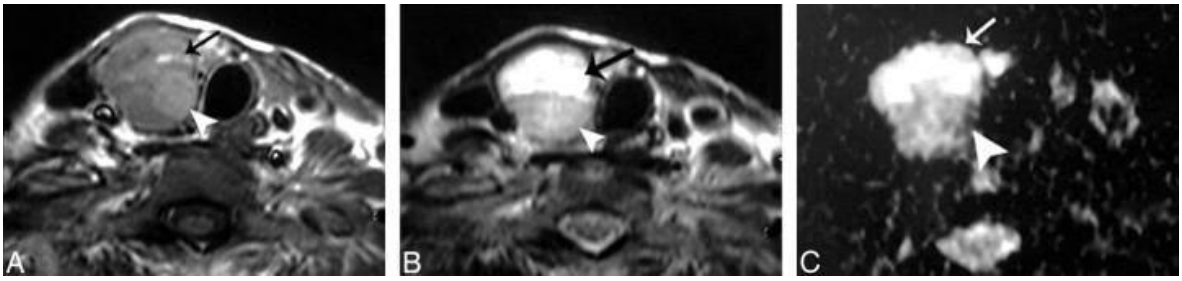

Figure 10: Follicular adenoma is a kind of adenoma shown in the Axial T1- and T2- weighted MR scans of a well-defined more or less oval solitary nodule affecting the right thyroid lobe with contralateral tracheal displacement, shown in A and B, respectively. The nodule has a cystic section in the front (arrow) and a solid part in the back (arrowhead). C. An ADC map image with marked hyperintensity of the anterior cystic portion of the nodule (arrow) indicates increased diffusion with a measured ADC value of 2.25 x 10^{-3} mm^2/s, and a relatively hypointense posterior solid portion (arrowhead) indicates relatively restricted diffusion with a measured ADC value of 1.2 x 10^{-3} mm^2/s.[58]

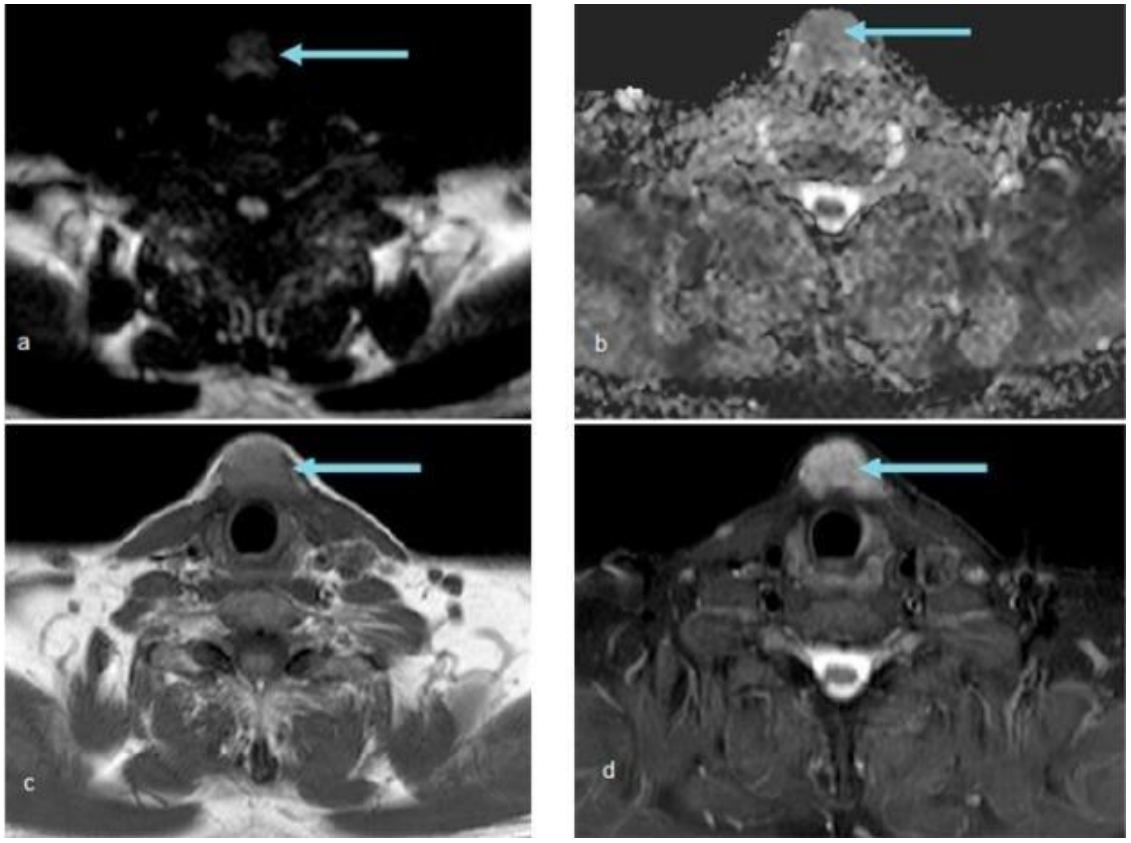

Figure 11: (a–d) MRI images (a) Axial DWI (b) Axial ADC map (c) Axial T1WI (d) Axial STIR. These images show recurrent thyroid nodule (arrows) demonstrating low T1 and high STIR signal intensity with restricted diffusion seen as intermediate signal intensity in the DWI and low signal intensity in the ADC map with a mean ADC value reading 1 x 10^{-3} mm^2/s.[59]

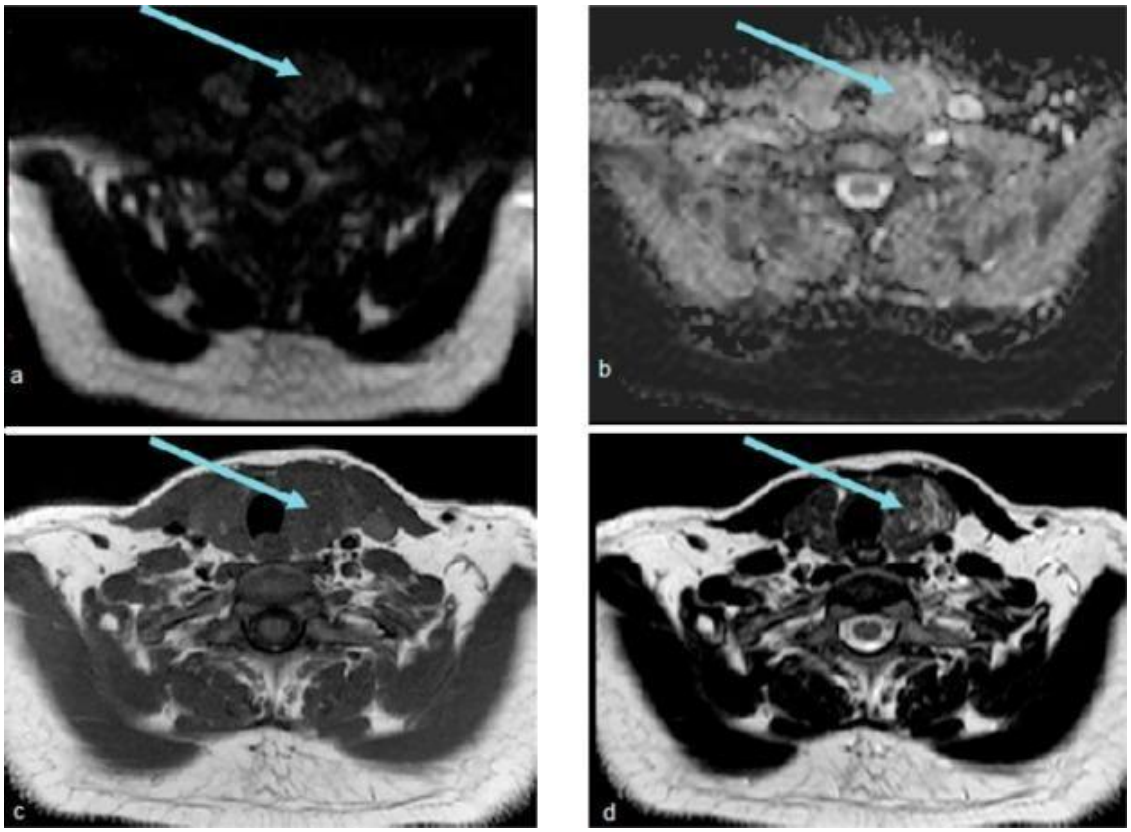

Figure 12: (a–d) MRI images (a) Axial DWI (b) Axial ADC map (c) Axial T1WI (d) Axial T2WI. These images show left thyroid nodules (arrows) demonstrating intermediate in homogenous T1 and T2 signal intensity with facilitated diffusion seen as low signal intensity in the DWI and intermediate signal intensity in the ADC map with a mean ADC value reading 1.5×10^{-3} mm^2/s.[59]

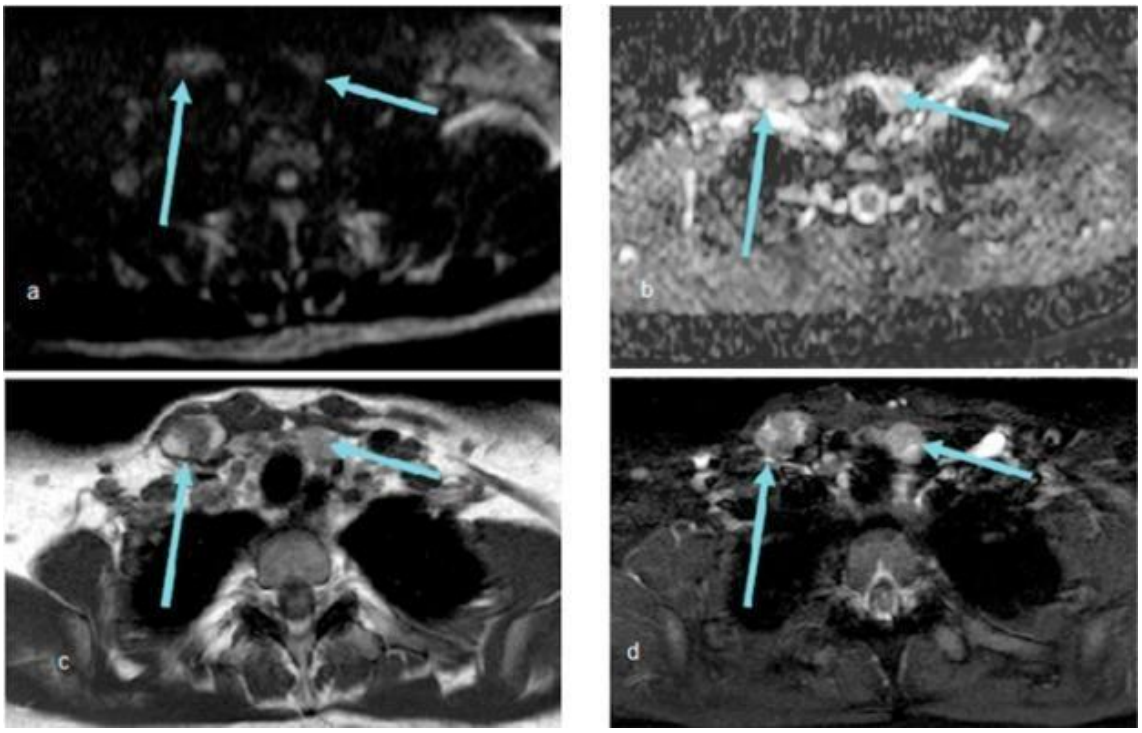

Fig 13: (a–d) MRI images (a) Axial DWI (b) Axial ADC map (c) Axial T1WI (d) Axial STIR. These images show recurrent left thyroid nodule and right lower deep cervical lymphadenopathy (arrows) with a mean ADC value for the recurrent left thyroid nodule reading 1.8 x 10^{-3} mm^2/s.[59]

Cut off ADC value to distinguish benign from malignant nodules using DWI:

DWI is a type of functional MRI that is based on water molecule diffusion across the target tissue (i.e., tumour tissue). DWI can reveal important details about the underlying pathology, molecular composition and pathophysiological pathways.[53] The diffusion of water molecules is restricted in malignant tumours, resulting in a lower apparent diffusion coefficient (ADC); this difference in the ADC aids in the differentiating of malignant and benign tumours.[60] DWI has been proven in numerous studies to be capable of distinguishing benign from malignant thyroid nodules. [21,61]

Diffusion-weighted imaging can reveal more about a tissue's microstructure and physiological processes. The random migration of water protons is affected by changes in the distribution of intracellular organelles and macromolecules in tissues. Tissue ADC values vary depending on cellularity and histopathology. In Anderson's study malignant lesions in thyroid glands were found to have compact cellularity, which raised the nucleocyte-cytoplasmic ratio.[62] The extracellular space is reduced as a result of these microscopic pathogenic alterations, limiting the diffusional motion of water protons. On DWI sequences, reduced ADC values appear as a strong signal.

The sensitivity and specificity were 97.5 percent and 91.7 percent, respectively, when using an ADC value of 0.98 $x1.0^{-3}$ mm^2/s as a cut-off point to identify benign and malignant lesions, according to Abdel's study.[63] The accuracy was as high as 98.9%. A single pair of b values (0, 1000 s/mm^2) was investigated in this study. We also looked at ADC values obtained with higher b values (0,800 s/mm^2), but we couldn't find any useful thresholds at those b values. Our study focused on the thyroid, whereas Abdel's study included a range of cervical lymph nodes. The discrepancies in sensitivity could have been due to lesion heterogeneity. It was also proposed that the ADC values of benign thyroid nodules could differ depending on the

nodule's complex makeup (colloid, tiny necrosis, cystic change, hemorrhage, fibrosis and calcium). Thyroid cysts had the highest ADC values because they contained a serous colloid cyst.

Thyroid nodules were also examined using DWI at lower b-values by Bozgeyik.[21] A b-factor of 300 s/mm^2 was also shown to be most useful for distinguishing benign from malignant lesions by Bozgeyik. The ADCs were computed using three b-value pairs in Bozgeyik's study: (0, 100 s/mm^2), (0, 200 s/mm^2), and (0, 300 s/mm^2). We followed up on these findings by looking at ADC values obtained with greater b-values. Erdem, also found that small calcification was linked to a decrease in ADC values in thyroid cancer patients.[22]

A contrasting result was found in Weidekamm's study[64,65]. With values equal to or greater than 2.25×10^{-3} mm^2/s, ADC values in malignant thyroid nodules were significantly higher than in benign nodules. The increased ADC values could be owing to an overabundance of thyroprotein follicles in malignant thyroid nodules, which do not prevent water protons from diffusing freely.

ADC readings have been utilized to distinguish between benign and malignant lesions as a quantitative metric.[66] Many factors influence ADC levels, including tissue architecture, necrosis, the presence of macromolecules and the perfusion phenomenon. When compared to benign lesions, malignant lesions have more aberrant blood perfusion and both blood perfusion and extracellular space affect ADC values. Unlike some previous investigations, Wu, Y et al.[2] used three distinct b factors: 0, 400 s/mm^2, and 800 s/mm^2 since ADC values with bigger b factors would better reflect real water diffusion in the tissue. When the b factors were 500 s/mm^2 and 800 s/mm^2, they discovered no significant difference in ADC value between benign and malignant tumours.

Delormere et al. showed that malignant lesions often lack a full basal membrane of the blood vessel which improves molecular exchange in the capillary bed.[67] Blood perfusion and extracellular space may both influence ADC levels. Increased blood perfusion enhances the apparent speed of diffusing water protons in thyroid cancer, whereas a restricted extracellular space restricts their mobility. With b-values of 500 s/mm^2 or 800 s/mm^2, our results show no difference in ADC values between benign and malignant groups, despite the fact that sensitivity to perfusion is diminished at higher b-values. Perfusion and diffusion effects are most likely influencing the ADC values obtained with the lower b-value of 300 s/mm^2. It's likely that the lower 300 s/mm$^{2'}$ discriminatory effect is due to a combination of increased vascularity and cellular composition changes that characterize malignancy.

4. MOST RELEVANT STUDIES:

A study by Fath El- Bab, Hytham, et al.[68] (2021) aimed to study and differentiate thyroid nodules on DWI by using the reference as a histopathological study which includes 35 patients (28 females and 7 males) their ages varies from 12 years to 75 years. The percentage of the benign nodule was 52.9%, and the malignant nodules were 47.1%. The range of ADC values for benign nodules were (0.03 to 3.5) value significant with a cut-off value of 1.2 with 93% sensitivity and 83% specificity. DWI provides very useful and promising results on the nature of a thyroid nodule.

Huang, Shengyi, et al.[69] (2021) study was performed to detect thyroid diseases at different levels by using dielectric properties of thyroid nodules. Open-ended coaxial was used as a method to measure dielectric permittivity of thyroid tissues for 155 patients at undergo frequencies ranging between 1-400MHz. Normal thyroid tissue, benign and malignant thyroid nodules were investigated by the pathological report. The analysis results revealed that the

dielectric permittivity and conductivity values positively correlated with the degree of malignancy of the nodule ($P < 0.05$).

A prospective study by **Bhargava, K et al.**[1] **(2020)** included a total of fifty patients with neck swelling diagnosed clinically and confirmed on ultrasound. The mean age of the patients was 41.8±13.9 years, with a maximum number of patients in the age group of 31 to 40 years. The mean ADC value of benign nodules ($1.721x10^{-3}mm^2$ /sec) was suggestively higher than that of malignant nodules ($1.075x10^{-3}mm^2$/sec) (p=0.01). The best cut-off value for distinguishing benign and malignant nodules was $1.37x10^{-3}mm^2$/sec with sensitivity, specificity, PPV and NPV of 93.75%, 91.17%, 83.33%, and 96.87%, respectively. The accuracy of the study in discriminating benign from malignant nodules was 92%.

Abdelgawad, Ehab Ali, et al.[70] **(2020)** assessed the utility of ADC value in discriminating different subtypes of single thyroid nodules using diffusion MRI with pathological correlation. It's a prospective study that included 73 patients. There was a substantial difference in ADC values between malignant and benign thyroid nodules with the mean ADC value for the benign group ($1.7 \pm 0.12 \times 10^{-3}$) increased as compared to malignant nodule ($0.71 \pm 0.15 \times 10^{-3}$). The sensitivity (97.5%), specificity (94.4%), and accuracy (94.4%) of ADC in differentiating different subtypes were present.

Mona A.M. Ali Nagi, M.D. et al.[71] **(2020)** study examined the accuracy of Diffusion Weighted Imaging (DWI) and ADC in distinguishing between benign and malignant thyroid nodules by using histopathology as a reference study. This study included 32 patients (19 females 59.4% and 13 males 59.4%) ages varying from 22-66 years and diagnosed by ultrasonography to have thyroid nodules. ADC values were able to differentiate benign from malignant thyroid disease.

Kong, Weidan, et al.[72] **(2019)** enrolled 100 subjects with 137 nodules examined for the operation with help of both DWI and ultrasound. The intensity ratio (SIR) of each thyroid nodule was calculated by measuring the mean intensity divided by that of paraspinal muscle. By using two simple independent tests, the ADC value, benign and malignant thyroid nodules, were analysed. The threshold value was $1.12 \times 10\text{-}^{3}$ mm^2/s; the maximum AUC was 0.944. The sensitivity, specificity, and accuracy were 84.9, 92.2, and 87.6%, respectively. The corresponding values of ultrasound diagnosis were 90.1, 80.4, and 86.9%. These results suggest both ultrasound and DWI to be helpful in differentiating benign and malignant thyroid lesions.

Linh, Le Tuan et al.[57] **(2019)** used ultrasound imaging and magnetic resonance imaging to assess thyroid nodules (MRI). The study included 93 participants who had been diagnosed with 128 thyroid nodules and had surgery. The ADC value was determined for each b value using the statistical tool (spss software). The mean ADC value of the malignant group ranged from 200 to 800, which was significantly greater than the benign group. With improved precision, the ADC cut-off value for discriminating malignant from benign thyroid lesions is 1.7×10^{-3} mm^2/s (87.1 percent, 95 percent CI: 79.59-92.07 percent).

Ahmed Mohamed et al.[59] **(2018)** conducted a study on the potential application of diffusion-weighted imaging in differentiating benign and malignant thyroid nodules. The retrospective study was regulating on 30 patients (10 Males & 20 Females); the ages varied from 29 to73 years. Malignancy was reported in 56.7% and was not in 43.3% of patients. Statistical analysis of this study found that ADC values significantly decreased ($P < 0.001$) in malignant lesions. The ADC cut-off value differentiating the benign and malignant lesions was 1.15; this cut-off had 88.2% and 92.3% sensitivity and specificity, respectively. Hence, these results concluded that MRI-DWI plays a useful role in thyroid nodules and recurring nodules after

thyroidectomy by providing a good determining tool for measurement of the ADC value, differentiating between benign and malignant nodules.

Leila Aghaghazvini et al.[73] **(2018)** involved 41 thyroid nodules in the research (26 benign and 15 malignant), mean ADC value being (1.94 0.54) x 10^{-3} mm^2/s and (0.89 0.29) x 10^{-3} mm^2/s respectively (P-value 0.005). To distinguish benign and malignant nodules, an ADC value cutoff of 1 x10^{-3} mm^2/s showed accuracy, sensitivity, and specificity of 93 percent, 87 percent, and 96 percent, respectively.

O, Ekinci et al.[74] **(2018)** study involved 58 patients. The benign nodules account for 50 (76.9%) of the total, while the malignant nodules account for 15 (23.1%). The malignancy group had substantially lower minimum, maximum, and mean ADC values of the nodules (p 0.05). With a sensitivity of 66.67 percent, a specificity of 89.13 percent, a positive predictive value of

53.63 percent, and a negative predictive value of 89.13 percent, the optimal cut-off value for the mean ADC value was 1.33 x 10-3 mm^2/s. A mean ADC value of less than or equal to 1.33 x 10^{-3} mm^2/s was linked to 9-fold increased risk of cancer.

A prospective study by **Abdel-Rahman, Hossam M, et al.**[75] **(2016)** involved 60 patients in discriminating between malignant and benign thyroid nodules; a threshold value of 1.5 x 10^{-3} mm^2/s was used. As a result, the researchers came to the conclusion that DWI is a good way to tell the difference between benign and malignant nodules.

A meta-analysis by **Lihua Chen et al.**[76] **(2016)** comprised 765 lesions in total, 113 recognized search results, and 15 papers. The diagnostic 150.73 had a collective weighted sensitivity of 0.90; the specificity was 0.95, the positive ratio was 16.49 and the negative

ratio was 0.11. The RO characteristic curve's AUC was 0.95. DWI can be a non-invasive, radiation-free, and precise means of distinguishing between malignant and benign tumours.

Abd el Aziz et al.[77] **(2015)** study involved 61 patients (15 males and 46 females) with ages varying between 30–70years. ADC values were established for individual b-values. The values of the ADC of thyroid nodes and histopathology were compared. The pathology results found 38 benign and 23 malignant thyroid nodules. ADC value for b-values of 0–300s/mm^2 was used to evaluate benign and malignant thyroid nodules, which were significant ($p<0.001$). Increased ADC values were seen in benign nodules (ADC: $2.32\pm0.44\times10^{-3}mm^2/s$) than malignant ones ($1.40\pm0.40\times10^{-3}mm^2/s$).

LM, Wu et al.[78] **(2014)** study assessed diffusion-weighted magnetic resonance (DWI) imaging's ability to differentiate malignant thyroid nodules from benign lesions using meta-analysis. By the statistical analysis, pooled estimation and subgroup analysis data are obtained. The study includes 358 patients, and seven studies (17 subsets) with all inclusion criteria were considered for the analysis. DWI sensitivity was 0.91 (95% confidence interval [CI], 0.87-

0.94) and specificity was 0.93 (95% CI, 0.86-0.96). All together positive ratio 12.24 (95% CI, 6.47-23.20) and negative ratio 0.99 (95% CI, 0.06-0.15). The diagnostic odds ratio was 123.78 (95% CI, 56.85-269.48). The summary of ROC was 0.94 (95% CI, 0.92-0.96). When a patient's pre-test probabilities increased, DWI enabled confirmation, and in decreased DWI enabled exclusion of malignant thyroid lesion. Worst-case post-test probabilities were 92% and 9% for positive and negative, respectively.

A study by **Wu, Yingwei, et al.**[2] **(2013)** aimed to assess the usefulness of diffusion-weighted imaging in distinguishing malignant tumours from thyroid lesions. The study included 42

patients, 10 males, and 32 women, ranging in age from 20 to 72 years. Multiple b-values were used in routine neck MR, ADC, and diffusion-weighted MR imaging. A histological outcome of the thyroidectomy samples were obtained for all individuals. The ADC values in benign lesions were substantially higher (benign ADC: 2.37±0.47 x 10^{-3} mm^2/s vs. malignant ADC:

1.49±0.60 x 10^{-3} mm^2/s). The two most discriminative metrics for discriminating malignancy were ADC values derived with b-values of 0 and 300 mm^2/s and maximum nodular diameter.

A prospective study by **Shi, Hai Feng, et al.**[79] **(2013)** involved a total of 111 subjects with single thyroid nodules (23 malignant and 88 benign nodules) who underwent DWI MRI. On DWI, the majority of malignant thyroid nodules (65%) were mildly hyperintense, while the majority of benign nodules (69%) were hyperintense (P 0.01). The ADC levels in thyroid cancer were lower than in adenoma and nodular goitre (P 0.05). An ADC value of 1.704x10^{-3} mm^2/s can be used as a threshold to distinguish benign from malignant nodules when the b factor is 500 s/mm, with 92 percent sensitivity, 88 percent specificity, and 87 percent accuracy. Thyroid cancer has a lower ADC value due to the increased cell density.

Mutlu, Hakan, et al.[80] **(2012)** study was conducted on 44 patients (27 females, 17 males). The images were acquired with 0, 50, 400, and 1000 s/mm b values. The ADC ratio is calculated in the DW images, 0.27 in benign and 0.86 in malignant lesions. The threshold value was calculated as 0.56 according to the ROC analysis. This threshold value showed sensitivity 100%, specificity 97%, positive predictive value 83%, negative predictive value 100%, and accuracy rates 98% in distinguishing benign from malignant thyroid lesions. They found that the ADC ratio has increased values for sensitivity and specificity among the tests defined for characterization of nodules.

A Dilli et al.[81] **(2012)** study assessed the effectiveness of the ADC calculated in distinguishingbetween benign and malignant thyroid nodules. It was a prospective study that included 52 patients. Diffusion-weighted echo-planar imaging was performed, and b factors were taken as 0 and 400 s/mm^2. Malignant thyroid nodules had an ADC of 0.8290.179 x 10^{-3} mm^2/s, while benign thyroid nodules had an ADC of 1.9840.482 x 10^{-3} mm^2/s.[86]

Erdem, Gulnur, et al.[22] **(2010)** study enrolled 52 patients with thyroid nodules. The mean ADC values of thyroid nodules were 2745.3 ± 601.1 × 10^{-6} mm^2/s (1605-3899 × 10^{-6} mm^2/s) in the benign group and 695.2 ± 312.5 × 10^{-6} mm^2/s (165-1330 × 10^{-6} mm^2/s) in the malignant group. A reduced ADC was observed in most types of malignant tumours due to the consequent decrease of the extracellular extravascular space. Hence, results showed that ADC values of nodules may provide useful data about the nature of a thyroid nodule.

Bozgeyik, Zulkif, et al.[21] **(2009)** study included 93 patients thyroid nodules assessed using following b factors of 100, 200, and 300 mm^2/s. Mean ADC values for malignant and benign nodules for b 100 factor were 0.56 ± 0.43 × 10^{-3} and 1.80 ± 0.60 × 10^{-3} mm^2/s respectively. This shows that mean ADC values of malignant nodules were decreased as compared to benign nodules. ADC values among normal-appearing thyroid parenchyma of patients and healthy subjects were insignificant at all b factors. Hence, benign nodules have increased ADC values than malignant ones.

LACUNAE OF LITERATURE:

MRI with diffusion-weighted images has been used enormously in evaluating and diagnosing benign and malignant lesions in most of the organs. However, its use in thyroid lesions is not well established, although studied globally. ADC value strongly depends on the b-value image, which means ADC images are separately developed with different b values. The ADC

values represent the tissue's diffusion restriction properties. All of the current studies have one point of view in common: the authors tout the benefits of diffusion-weighted imaging (on machines with a strong magnetic field), which can accurately estimate the ADC value. To distinguish between malignant and benign thyroid lesions, a suitable cut-off point for ADC values must be established. However, the authors have yet to achieve an agreement on a number of topics, including how to choose the best b value for a thyroid MRI and the associated recommended cut-off ADC value to detect a cancerous nodule. Furthermore, there is fewer research done in India on the use of the ADC value in thyroid nodules.

MATERIAL & METHODS

MATERIALS AND METHODS:

Study site: This study was performed in the Department of Radio-diagnosis at R.L Jalappa Hospital and Research center attached to SDUMC, Kolar.

Study population: All the eligible patients who would have undergone MRI at the Department of Radio-diagnosis at R.L Jalappa Hospital and Research center were considered as the study population.

Study design: The present study was a hospital-based observational study.

Sample size: Sample size estimated by using the proportion of patients with benign and malignant thyroid nodules detected by DWI from the study by Aghaghazvini L et al.[73] using the formula:

Formula

$$n = \frac{z^2_{1-\frac{\alpha}{2}} p(1-p)}{d^2}$$

Where,

p : Sensitivity of the new test

d : precision

$Z_{1-\alpha/2}$: Desired Confidence level

Here

Z1-α/2 = 1.96 at 5 % error alpha. As in the majority of studies, *p* values are considered significant below 0.05; hence 1.96 is used in the formula.

P = Expected proportion in population based on previous studies or pilot studies.

d = Absolute error or precision – has to be decided by researcher.

p = 0.87

1 – p = 0.13

d = 10 %

Assuming sensitivity of 87 % with absolute precision of 10 %, confidence interval of 95 %, the minimum sample size was found to be 43.

Sampling method: Until the sample size was met, all eligible subjects were sequentially recruited into the study using easy sampling.

Study duration: The data collection for the study was done between January 2020 to June 2021 for a period of 18 Months.

Inclusion Criteria:

1. Patients with thyroid swelling/nodule on clinical examination.
2. Patients with thyroid swelling/nodule on ultrasonographic examination.

Exclusion criteria:

1. Patients in whom fine needle aspiration or previous instrumentation or biopsy has been done within the last 3 weeks.

Ethical considerations: The study was approved by the institutional human ethics committee. Informed written consent was obtained from all the study participants, and only those participants willing to sign the informed consent were included in the study. The risks and benefits involved in the study and the voluntary nature of participation were explained to the participants before obtaining consent. The confidentiality of the study participants was maintained.

Data collection tools: Patients with clinically palpable thyroid nodules who undergo MRI neck were included in the study if they fulfil the inclusion/exclusion criteria. Written Informed Consent was taken for their willingness to participate in the study. Baseline data were collected from the patients along with pertinent clinical history and relevant lab investigations.

METHODOLOGY:

MRI neck was performed using a 1.5 T 18 channel MR Scanner (Siemens® Magnetom Avanto®).Axial turbo spin-echo T2-weighted (TR/TE: 2500/75, matrix size of 307 × 384, FOV: 220 mm, and slice thickness = 4 mm with intersection gap = 1 mm), coronal turbo spin-echo T2-weighted (TR/TE: 3000/69, matrix size of 307 × 384, FOV: 240 mm, and slice thickness = 5 mm with intersection gap = 1 mm), and axial T1-weighted (TR/TE: 746/11, matrix size of 307 × 384, FOV: 220 mm, and slice thickness = 4 mm with intersection gap = 1 mm) images were obtained. Diffusion-weighted imaging was obtained in the axial plane by single-shot spin-echo echo-planar imaging at b values of 0, 400 and 800 (TE: 70, TR: 5400, slice thickness: 4 mm with no intersection gap and the number of signal acquisition). After acquiring images, regions of interest were drawn in every suspected nodule on DWI images based on the size of the nodule excluding areas of calcification, necrosis or cystic components.

STATISTICAL METHODS:

HPE and ADC values were considered as primary outcome variables. Size, shape, margins, and composition of the lesion, T1 weighted imaging and T2 weighted MRI imaging findings, ADC values of the lesions, extrathyroidal invasion, and status of lymph nodal involvement were considered as other study relevant variables.

For quantitative variables, mean and standard deviation were used, whereas, for categorical variables, frequency and proportion were used. The median and interquartile range were used to summarize non-normally distributed quantitative values (IQR). Data was also shown using relevant diagrams such as bar graphs and pie graphs.

Visual inspection of histograms and normality Q-Q plots were used to assess all quantitative variables for normal distribution within each category of the explanatory variable. To

determine normal distribution, the Shapiro-Wilk test was used. Normal distribution was defined as a p-value of >0.05 in the Shapiro-Wilk test.

Categorical outcomes were compared between study groups using the Chi-square test /Fisher's Exact test (If the overall sample size was < 20 or if the expected number in any one of the cells is < 5, Fisher's exact test was used.).

ROC analysis: The utility of the ADC value of the thyroid nodule in predicting histopathological diagnosis of the nodule was assessed by Receiver Operative curve (ROC) analysis. The area under the ROC curve, along with its 95% CI and p-value, are presented. Based on the ROC analysis, it was decided to consider 1.0×10^{-3} mm^2/s as the cut-off value. The specificity, sensitivity, diagnostic accuracy, and predictive values and of the screening test with the decided cut-off value along with their 95% CI are presented.

P-value < 0.05 was considered statistically significant. Data were analyzed by using SPSS software, V.22.[82]

RESULTS

OBSERVATIONS AND RESULTS

A total of 43 subjects were included in the final analysis.

Table 1: Descriptive analysis of age in study population (N=43)

Parameter	Mean ± SD	Median	Minimum	Maximum
Age	49.88 ± 14.38	50	24	78

The mean age was 49.88 ± 14.38 years, ranged between 24 to 78 years in the study population. (Table 1)

Table 2: Descriptive analysis of gender distribution in the study population (N=43)

Gender	Frequency	Percentages
Male	8	18.60%
Female	35	81.40%

Among the study population, 8 (18.60%) participants were male, and 35 (81.40%) were female. (Table 2 & Figure 14)

Figure 14: Pie chart showing gender distribution in the study population (N=43)

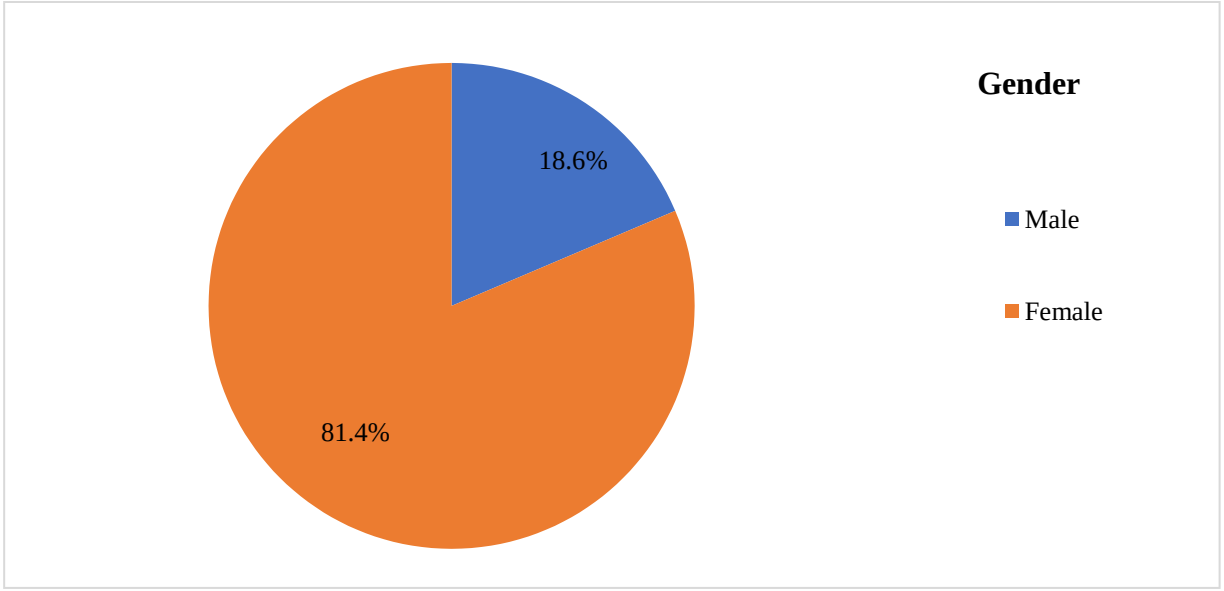

Table 3: Descriptive analysis of side (lobe) of involvement in the study population (N=43)

Side (Lobe) Of Involvement	Frequency	Percentages
Left	16	37.21%
Right	13	30.23%
Both	12	27.90%
Isthmus	1	2.33%

Among the study population, 16 (37.21%) participants had involvement of the left thyroid lobe, 13 (30.23%) participants had right thyroid lobe involvement, 12 (27.90%) had both lobes involved, and only 1 (2.33%) had isthmus involvement. (Table 3 & Figure 15)

Figure 15: Bar chart showing side (lobe) of involvement in the study population (N=43)

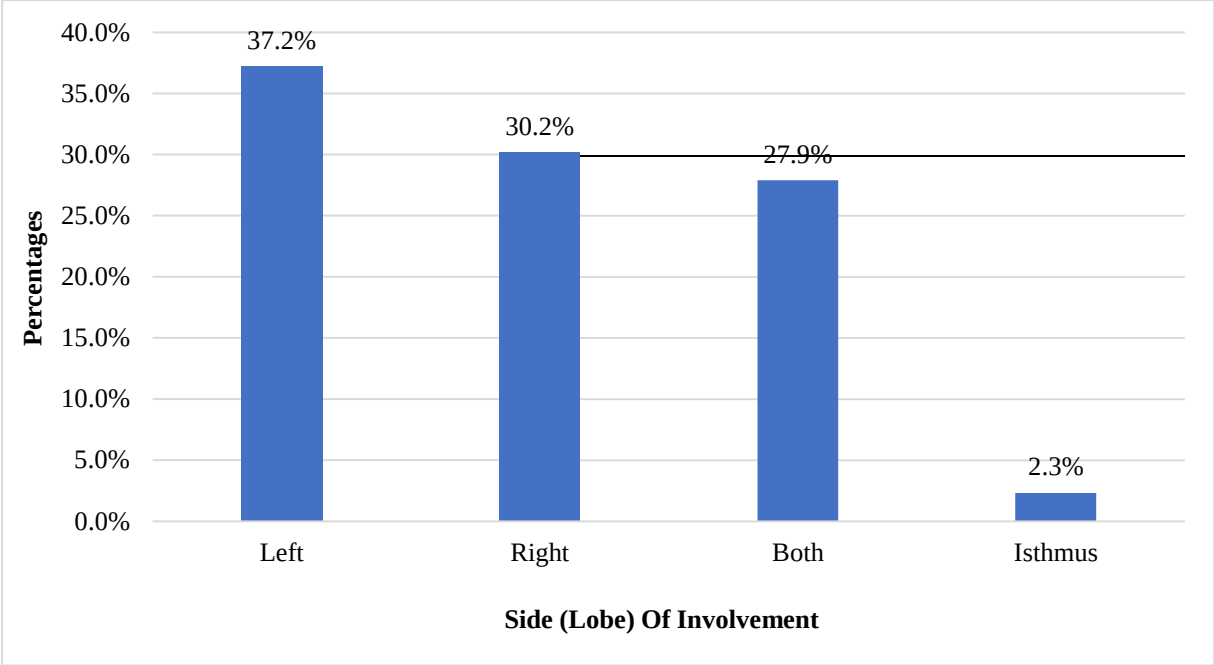

Table 4: Descriptive analysis of number of nodules in the study population (N=43)

Number of nodules	Frequency	Percentages
One	24	55.81%
Two	5	11.63%
Multiple	14	32.56%

Among the study population, 24 (55.81%) were reported as having one nodule, 5 (11.63%) were reported having two nodules, and 14 (32.56%) were reported having multiple nodules. (Table 4 and Figure 16)

Figure 16: Pie chart showing number of nodules in the study population (N=43)

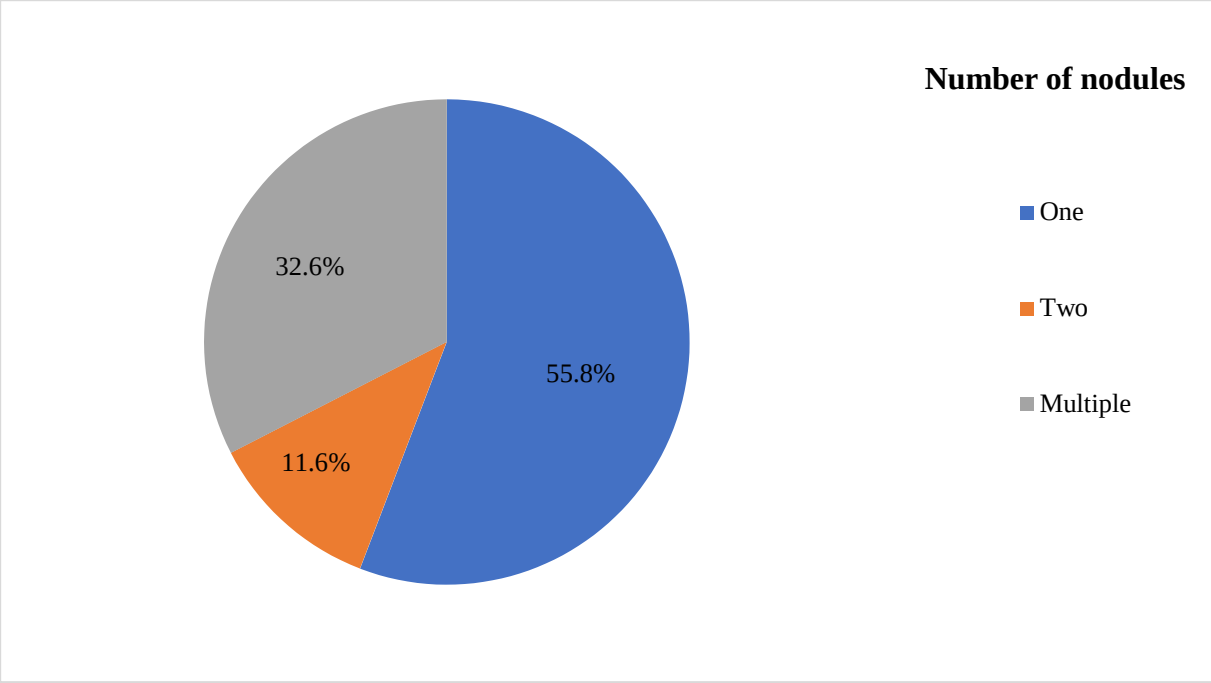

Table 5: Descriptive analysis of the shape of the nodules in the study population (N=43)

Shape	Frequency	Percentages
Round	25	58.14%
Oval	12	27.91%
Irregular	6	13.95%

Overall, 25 (58.14%) participants had a round shape of the nodule, 12 (27.91%) had an oval shape, and 6 (13.95%) had an irregular shape of the nodule. (Table 5 and Figure 17)

Figure 17: Bar chart showing the shape of the nodule in the study population (N=43)

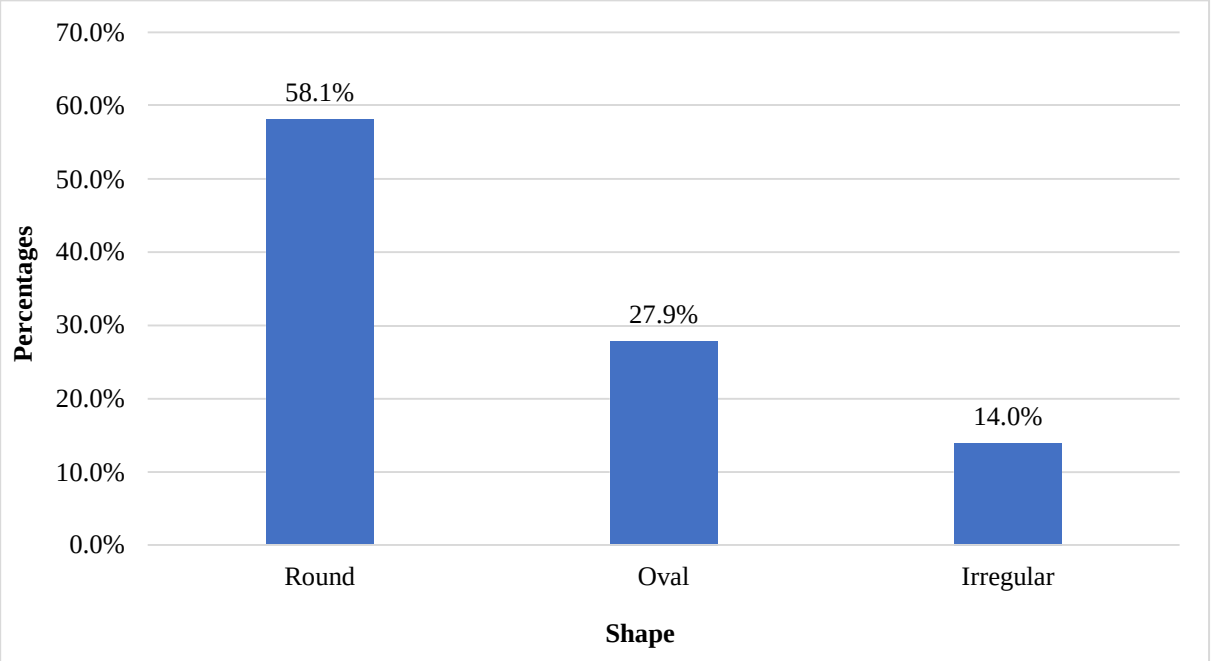

Table 6: Descriptive analysis of margins of the nodule in the study population (N=43)

Margins	Frequency	Percentages
Smooth	35	81.40%
Irregular	6	13.95%
Lobulated	2	4.65%

Overall, 35 (81.40%) participants had nodules with smooth margin, 6 (13.95%) had nodules with irregular margin, and 2 (4.65%) had nodules with lobulated margin. (Table 6 & Figure 18)

Figure 18: Pie chart showing margins of the nodule in the study population (N=43)

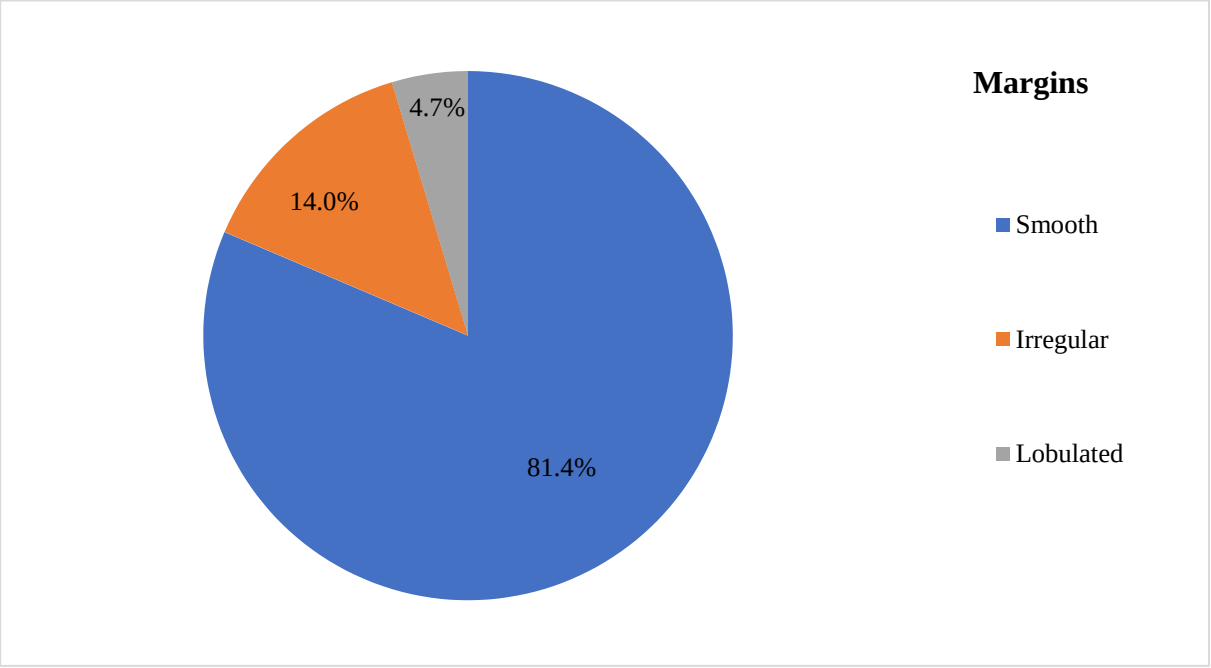

Table 7: Descriptive analysis of the composition of the nodule in the study population (N=43)

Composition of the lesion	Frequency	Percentages
Predominantly cystic	3	6.98%
Predominantly solid	8	18.60%
Solid-cystic	9	20.93%
Solid	23	53.49%

Out of 43 participants, 23 (53.49 %) had nodules with solid composition, 9 (20.93 %) had nodules with solid-cystic composition, 8 (18.60 %) had nodules with predominantly solid composition, and 3 (6.98 %) had nodules with predominantly cystic composition. (Table 7 & Figure 19)

Figure 19: Bar chart showing the composition of the nodule in the study population (N=43)

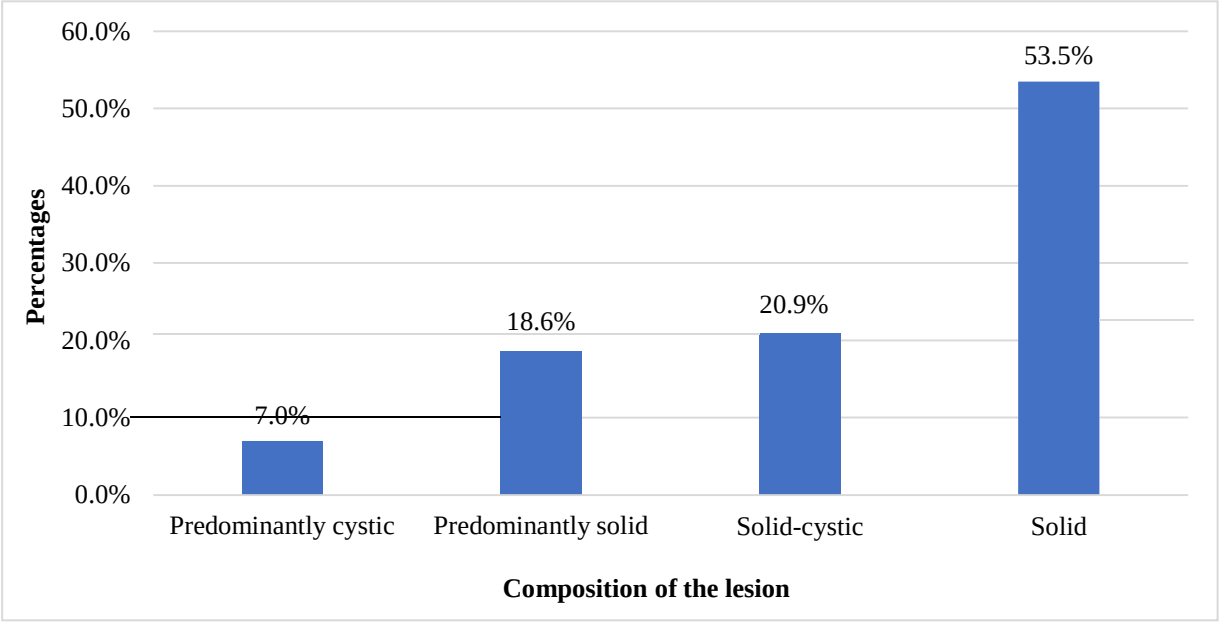

Table 8: Descriptive analysis of extrathyroidal extension of the thyroid nodule in the study population (N=43)

Extrathyroidal Extension	Frequency	Percentages
Retrosternal	1	2.33%
Nil	42	97.67%

Out of 43 participants, only 1 (2.33%) had a retrosternal extension of the thyroid lesion. (Table 8)

Table 9: Descriptive analysis of the presence of calcifications within the nodule in the study population (N=43)

Calcifications	Frequency	Percentages
Present	5	11.63%
Nil	38	88.37%

Out of 43 participants, 5 (11.63%) participants had thyroid nodules showing calcifications within. (Table 9)

Table 10: Descriptive analysis of the involvement of lymph nodes in the study population (N=43)

Lymph Nodes	Frequency	Percentages
Present	9	20.93%
Nil	34	79.07%

Out of 43 participants, 9 (20.93%) participants had lymph nodal involvement. (Table 10)

Table 11: Descriptive analysis of diffusion-weighted imaging findings of the thyroid nodules in the study population (N=43)

DWI	Frequency	Percentages
Restricting	9	20.93%
Non-Restricting	34	79.07%

Among 43 participants, 9 (20.93%) of them had thyroid nodules showing restricted diffusion, and 34 of them had thyroid nodules which were not showing restricted diffusion on DWI with ADC. (Table 11 and Figure 20)

Figure 20: Pie chart showing diffusion-weighted imaging findings of thyroid nodules in the study population (N=43)

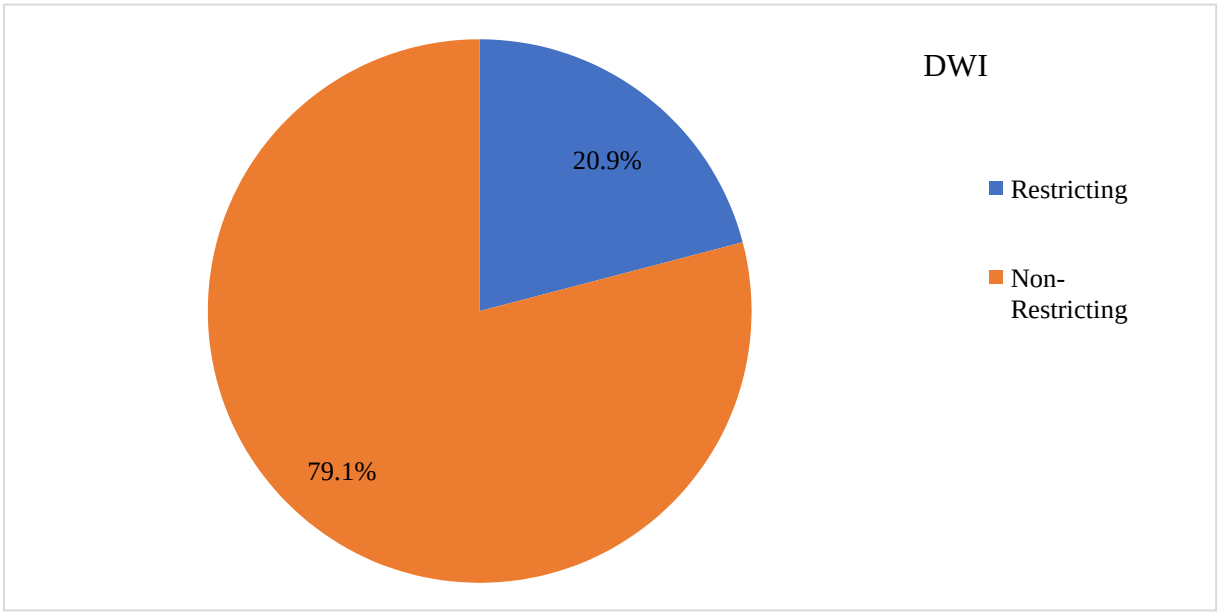

Table 12: Descriptive analysis of ADC value of the thyroid nodules in study population (N=43)

Parameter	Mean ± SD	Median	Minimum	Maximum
ADC value	1.42 ± 0.45	1.40	0.51	2.90

The mean ADC value of thyroid nodules is obtained as 1.42 ± 0.45 x 10^{-3} mm^2/s, ranging between 0.51 to 2.90 x 10^{-3} mm^2/s. (Table 12)

Table 13: Descriptive analysis of pathological findings of the thyroid nodules in the study population (N=43)

Pathological Findings	Frequency	Percentages
Nodular hyperplasia	11	25.58%
Lymphocytic thyroiditis	7	16.28%
Colloid nodule	6	13.95%
Hashimoto's thyroiditis	5	11.63%
Benign follicular lesion	4	9.30%
Papillary thyroid carcinoma	4	9.30%
Anaplastic carcinoma	2	4.65%
Follicular carcinoma	2	4.65%
Adenomatoid nodule with cystic change	1	2.33%
Hyalinizing trabecular adenoma	1	2.33%

Among 43 participants with 43 thyroid nodules considered, 11 (25.58%) of them had thyroid nodules which were reported as nodular hyperplasia, followed by lymphocytic thyroiditis seen in 7 (16.28%) participants and Hashimoto’s thyroiditis in 5 (11.63%) participants. (Table 13)

Table 14: Descriptive analysis of final MRI diagnosis of the thyroid nodule in the study population (N=43)

MRI Findings	Frequency	Percentages
Malignant	8	18.60%
Benign	35	81.40%

In MRI diagnosis, 8 (18.60%) were malignant, and 35 (81.40%) were benign. (Table 14)

Table 15: Descriptive analysis of final histopathological diagnosis of the thyroid nodules in the study population (N=43)

Histopathological Diagnosis	Frequency	Percentages
Benign	35	81.40%
Malignant	8	18.60%

In HPE diagnosis, 35 (81.40%) were malignant, and 8 (18.60%) were benign. (Table 15)

Figure 21: ROC analysis of Predictive validity of ADC value of the thyroid nodules in predicting final HPE diagnosis of the thyroid nodules (N=43)

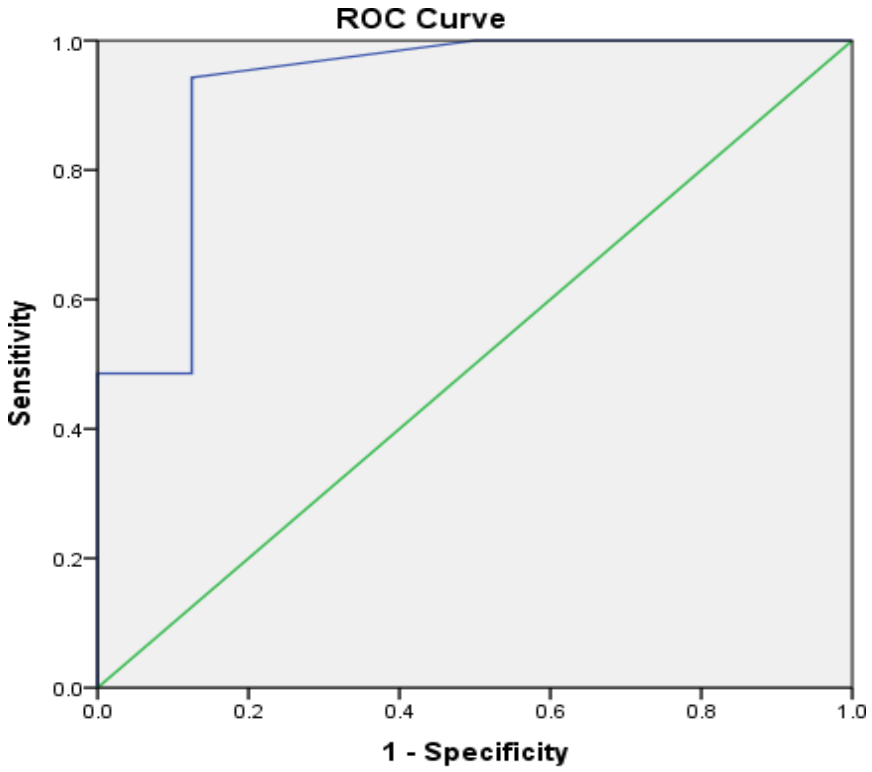

Test Result Variable(s): ADC				
Area Under the Curve	**Std. Error**	**Asymptotic 95% Confidence Interval**		**P-value**
		Lower Bound	**Upper Bound**	
0.925	0.062	.804	1.000	<0.001

The ADC value of thyroid nodules had excellent predictive validity in predicting malignancy, as indicated by the area under the curve of 0.925 (95% CI 0.804 to 1.000, P-value <0.001). (Figure 21)

Table 16: Comparison of histopathological diagnosis with ADC value (Considering 1 x 10^{-3} mm^2/s as mean ADC value**) (N=43)**

ADC Value	Histopathological Diagnosis		Chi square	P value
	Malignant (N=8)	Benign (N=35)		
Low (<1)	7 (87.5%)	2 (5.71%)	26.318	<0.001
High (>=1)	1 (12.5%)	33 (94.29%)		

Among 43 participants with 43 thyroid nodules considered, 8 were malignant, and 35 were benign, according to the HPE findings. Out of 8 malignant thyroid nodules, 7 (87.5%) participants showed thyroid nodules with ADC value <1.15 x 10^{-3} mm^2/s and only 1 (12.5%) had ADC value >=1.15 x 10^{-3} mm^2/s. Out of 35 benign thyroid nodules, 2 (5.71%) participants had thyroid nodules with ADC value <1.15 x 10^{-3} mm^2/s and 33 (94.29%) participants had thyroid nodules with ADC value >=1.15 x 10^{-3} mm^2/s. The difference in the proportion of HPE findings between ADC values of the thyroid nodules was statistically significant (P-value <0.001). (Table 16 & Figure 22)

Figure 22: Cluster bar chart showing a comparison of ADC value of thyroid nodules with histopathological diagnosis. (N=43)

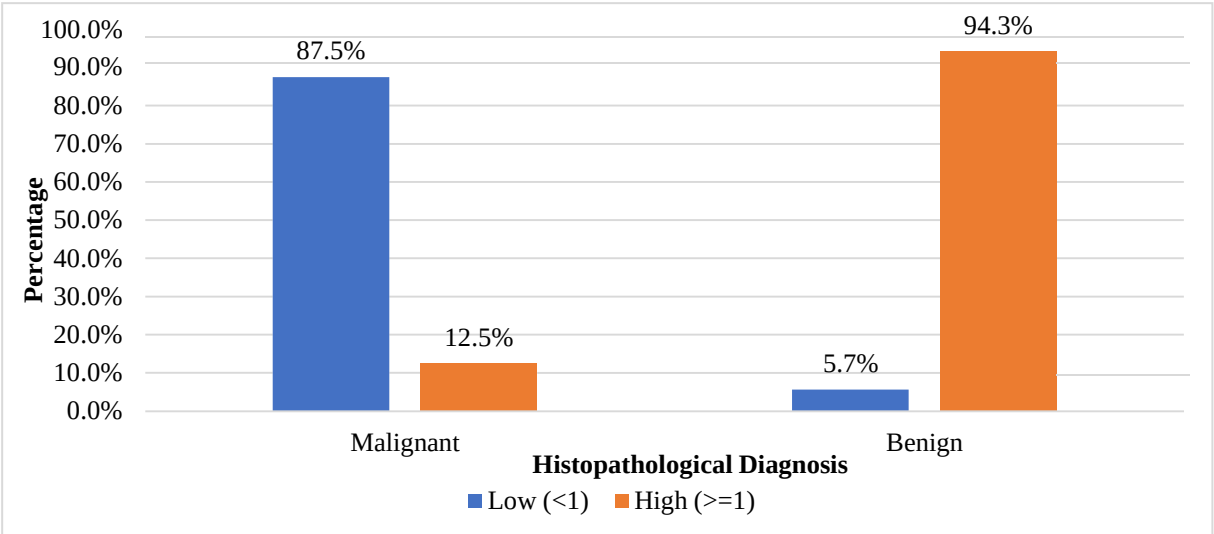

Table 17: Predictive validity of ADC value of the thyroid nodules in predicting Histopathological diagnosis. (N=43)

Parameter	Value	95% CI	
		Lower	Upper
Sensitivity	87.50%	47.35%	99.68%
Specificity	94.29%	80.84%	99.30%
False positive rate	5.71%	0.70%	19.16%
False negative rate	12.50%	0.32%	52.65%
Positive predictive value	77.78%	39.99%	97.19%
Negative predictive value	97.06%	84.67%	99.93%
Diagnostic accuracy	93.02%	80.94%	98.54%

The ADC cut off value of 1.15 x 10^{-3} mm^2/s had sensitivity of 87.50% (95% CI 47.35% to 99.68%) in predicting final HPE malignancy. Specificity was 94.29% (95% CI 80.84% to 99.30%), false positive rate was 5.71% (95% CI 0.70% to 19.16%), false negative rate was 12.50% (95% CI 0.32% to 52.65%), positive predictive value was 77.78% (95% CI 39.69% to 97.19%), negative predictive value was 97.06% (95% CI 84.67% to 99.93%), and the total diagnostic accuracy was 93.02% (95% CI 80.94% to 98.54%). (Table 17)

DISCUSSION

DISCUSSION:

The normal ultrasound features of thyroid parenchyma include a fine echotexture, iso-echogenicity, a smooth margin, a normal glandular size and normal parenchymal vascularity.[7,8] The recognized CT features of normal thyroid parenchyma include isoattenuation, homogeneous attenuation, an anteroposterior diameter of 1–2 cm, smooth border, and homogeneous enhancement.[83] Iso-/slightly enhanced SI on T1/T2-weighted images, homogeneous SI, normal anteroposterior diameter of the thyroid gland, smooth border, and homogeneously increased enhancement are all common MRI findings of normal thyroid parenchyma. Diffusion-weighted imaging has proved beneficial in discriminating benign and malignant thyroid lesions with ADC values, according to the literature. As a result, the goal ofthis study was to find a cutoff ADC value that might be used to distinguish benign from malignant nodules using DWI.

Our study involved 43 subjects, of which female participants (81.40%) were majority and male were 18.60%. Nearly 37.21% had left thyroid lobe, and 30.23% had right thyroid lobe, 27.90 % had both lobe and 2.33% had isthmus involvement. In the number of nodules involved, we found most of the study population to have a single nodule (55.81%) followed by multiple nodules in 32.56% and two nodules in 11.63% of the subjects. A similar study by Aghaghazvini L et al.[73] involved 41 thyroid nodules in 26 subjects, with the majority of subjects being females than males (f -73.07%, m-26.92%). A prospective study by Kanika B et al.[1] involved 50 subjects, with the female proportion being 74% and the male proportion being 26%.

The majority (58.14%) of the thyroid nodules had a round shape, 27.91% had an oval shape, and 13.95% had an irregular shape of the nodule. Most of the nodules (81.40%) exhibited smooth margin, irregular margin was found in 13.95%, and the lobulated margin was seen in 4.65%.

Among 43 subjects, the majority, 53.49% had nodules with solid composition, 20.93 % had solid-cystic composition, 18.60 % had a predominantly solid composition, and 6.98 % had predominantly cystic composition.

Among the study population, only 2.33% had a retrosternal extension of the thyroid lesion, 11.63% had thyroid nodules demonstrating calcifications within, and 20.93% participants had lymph nodal involvement.

Among 43 subjects, 20.93% of them had thyroid nodules showing restricted diffusion, and 79.06% of them had thyroid nodules that did not show restricted diffusion on DWI with ADC. The mean ADC value of thyroid nodules is obtained as $1.42 \pm 0.45 \times 10^{-3}$ mm^2/s, ranging between 0.51 to 2.90×10^{-3} mm^2/s. In a study by Kanika B et al.[1] out of 50 subjects taken into the study, 36% subjects showed diffusion restriction on DWI and had ADC value < than 1.371×10^{-3} mm^2 /sec (cut-off value), and 70% of subjects did not show restriction on DWI and had ADC > than $1.371 \times 10^{-3} mm^2$ /sec.

Among 43 subjects with 43 thyroid nodules considered, 25.58% had thyroid nodules which were reported as nodular hyperplasia, followed by lymphocytic thyroiditis in 16.28% participants and Hashimoto's thyroiditis in 11.63% participants.

With respect to the MRI diagnosis, 8 (18.60%) thyroid nodules were malignant, and 35 (81.40%) were benign. Considering HPE, 8 (81.40%) thyroid nodules were malignant, and 35 (18.60%) were benign. Hence from these results, we recorded that thyroid nodules which were diagnosed as benign on HPE were also diagnosed as benign as per MRI findings, and nodules which were diagnosed malignant were considered malignant as per MRI findings as well. Therefore, according to our study, benignity/malignancy of thyroid nodules were corresponding according to both HPE diagnosis and MRI findings.

In the present study, based on HPE findings, among 43 subjects having 43 thyroid nodules, 35 were benign, and 8 were malignant. Out of 8 malignant thyroid nodules, 7 (87.5%) participants showed ADC value $<1.15 \times 10^{-3}$ mm^2/s and only 1 (12.5%) had ADC value $>=1.15 \times 10^{-3}$ mm^2/s. Out of 35 benign thyroid nodules, 2 (5.71%) participants had thyroid nodules with ADC value $<1.15 \times 10^{-3}$ mm^2/s and 33 (94.29%) participants had thyroid nodules with ADC value $>=1.15 \times 10^{-3}$ mm^2/s. The difference in the proportion of HPE findings between ADC values of the thyroid nodules was statistically significant (P-value <0.001). The degree of restriction relies on the microenvironment of the tissue. The values of ADC largely depend on the density of cells and perfusion of blood to the tissues. Malignancy of thyroid nodules represents dense cellularity, high nucleocyte–cytoplasmic ratio, and frequently with the nuclear cell membrane, which results in constraint in Brownian motion of water molecules in extracellular space and leads to reduced ADC value.[84] We found that among the thyroid nodules diagnosed as benign as per HPE, the majority of nodules had ADC values greater than 1, 94.29 %, and the remaining 5.71% of cases were found to have ADC values less than 1 like that of malignant nodules. However, among the malignant nodules majority (87. 5%) were found to have ADC values less than 1, and only 12.5% of them had ADC values greater than 1. Similar findings were found in a study by Erdem et al.[22] where they found significantly increased ADC values among benign thyroid nodules and

significantly decreased ADC values among malignant thyroid nodules compared to the normal thyroid parenchyma. In addition, a study by Razek et al.[58] showed an ADC cut-off value of 0.98 × 10^{-3} mm^2/s which resulted in an accuracy of 98.9% for discrimination between benign and malignant thyroid nodules. However, in our study, the ADC cut-off was 1.15 x 10^{-3} mm^2/s. Few other studies have shown variable ADC cut-off values; a study by Wu et al.,[2] done considering *b* factor of 300 s/mm^2, reported accuracy of 87.6% with ADC cut-off value of 2.17 × 10^{-3} mm^2/s. Further, an ADC cut-off value of 1.60 × 10^{-3} mm^2/s has also been suggested.[85,86]

Wu et al.[2] obtained DWI with b value of 300 s/mm^2 and reported an accuracy of 87.6% with an ADC cutoff of 2.17 × $10^{-3}mm^2/s$. Several studies have proposed a b value of 300 to be enough for the characterization of thyroid nodules. However, according to the meta-analysis by Chen et al.[76] using higher b values improves the strength of DWI for characterization of thyroid nodules. Similarly, in our study, we obtained ADC values with b values of 0, 400, and 800 s/mm^2. These results have shown wide inconsistency among several studies due to different study designs, particularly due to different b factors considered and have used T2 MRI, and few other studies have used 3 T MRI in differentiating malignant and benign thyroid nodules.

The ADC cut off value 1.15 x 10^{-3} mm^2/s had sensitivity of 87.50% (95% CI 47.35% to 99.68%) in predicting final HPE diagnosis, specificity was 94.29% (95% CI 80.84% to 99.30%), false- positive rate was 5.71% (95% CI 0.70% to 19.16%), false-negative rate was 12.50% (95% CI 0.32% to 52.65%), positive predictive value was 77.78% (95% CI 39.69% to 97.19%),negative predictive value was 97.06% (95% CI 84.67% to 99.93%), and the total diagnostic accuracy was 93.02% (95% CI 80.94% to 98.54%). A cross-sectional study by Aghaghazvini, L et al.[73] found the mean ADC value in benign lesions as 1.94 ± 0.54 × 10^{-3}

mm^2/s and in malignant was $0.89 \pm 0.29 \times 10^{-3}$ mm^2/s (P-value < 0.005). Based on ROC analysis, ADC cut-off of 1×10^{-3} mm^2/s resulted in an accuracy of 93% for discrimination between benign and malignant nodules (sensitivity: 87%, specificity: 96%, and PPV and NPV: 93%). They also found with ADC cut-off of 1.8×10^{-3} mm^2/s, the sensitivity of 100% was achieved, whereas, in a cut-off of 0.72×10^{-3} mm^2/s, specificity of 100% was seen. A prospective study by Kanika B et al.[1] used an ADC cut-off value of $1.371 \times 10^{-3} mm^2$ /sec in differentiating benign from malignant thyroid nodules with a sensitivity of 93.75% and specificity of 91.17%, respectively. Further, a study by Ilica et al.[87] showed an ADC cut-off value of 0.9×10^{-3} mm^2/s which resulted in sensitivity and specificity of 90% and 100%, respectively, for differentiation of malignant and benign thyroid lesions. The cut-off ADC values of these studies were in concordance to the present study in differentiating benign and malignant thyroid nodules. The ADC value of thyroid nodules in our study had excellent predictive validity in predicting malignancy, as indicated by the area under the curve of 0.925 (95% CI 0.804 to 1.000, P-value <0.001).

CONCLUSION

CONCLUSIONS:

- This study was a hospital based observational study involving 43 subjects, of which female participants (81.40%) were majority and male were 18.60%.
- Considering the number of nodules involved among the study population majority of them, that is, 24 participants (55.81%) had single nodules, multiple nodules in 14 participants (32.56%), and 5 (11.63%) had two nodules.
- The majority (58.14%) of the thyroid nodules had a round shape, 27.91% had an oval shape, and 13.95% had an irregular shape of the nodule.
- Most of the nodules (81.40%) exhibited smooth margins, 13.95% had irregular margins, and 4.65% had lobulated margins.
- Among 43 subjects, the majority (53.49%) had nodules with solid composition, 20.93 % had a solid-cystic composition, 18.60 % had a predominantly solid composition, and 6.98 % had predominantly cystic composition.
- Among the study population, only 1 patient (2.33%) showed retrosternal extension of the thyroid lesion, 11.63% had thyroid nodules showing calcifications within, and 20.93% of participants had lymph nodal involvement.
- Among 43 subjects, 20.93% of them had thyroid nodules showing restricted diffusion, and 34 of them had thyroid nodules which were not showing restricted diffusion on DWI with ADC.
- The mean ADC value of thyroid nodules is obtained as $1.42 \pm 0.45 \times 10^{-3}$ mm^2/s, ranging between 0.51 to 2.90×10^{-3} mm^2/s.
- Among 43 subjects with 43 thyroid nodules, 25.58% had thyroid nodules which were reported as nodular hyperplasia, followed by lymphocytic thyroiditis in 16.28% participants and colloid nodule in 13.95% of participants.

- As per MRI diagnosis, 8 (18.60%) were malignant, and 35 (81.40%) were benign. As per HPE diagnosis, 8 (18.60%) were malignant, and 35 (81.40 %) were benign.
- Based on HPE findings, among 43 subjects having 43 thyroid nodules, 35 were benign, and 8 were malignant. Out of 8 malignant thyroid nodules, 7 (87.5%) participants showed thyroid nodules with ADC value <1.15 x 10^{-3} mm^2/s and only 1 (12.5%) had ADC value >=1.15 x 10^{-3} mm^2/s. Out of 35 benign thyroid nodules, 2 (5.71%) participants had thyroid nodules with ADC value <1.15 x 10^{-3} mm^2/s and 33 (94.29%) participants had thyroid nodules with ADC value >=1.15 x 10^{-3} mm^2/s. The difference in the proportion of HPE findings between ADC values of the thyroid nodules was statistically significant (P-value <0.001).
- The ADC cut off value of 1.15 x 10^{-3} mm^2/s had a sensitivity of 87.50% in predicting the final HPE diagnosis of thyroid nodules. Specificity was 94.29%, and the total diagnostic accuracy was 93.02%.
- Therefore, the ADC value of thyroid nodules obtained had excellent predictive validity in predicting malignancy, as indicated by the area under the curve of 0.925 (95% CI 0.804 to 1.000, P-value <0.001).

SUMMARY

SUMMARY:

DWI is an MRI technique, which is non-invasive and helps in differentiating benign and malignant characteristics of the tissue. ADC is an objective parameter derived from DWI techniques, which helps to evaluate the tissue-specific diffusion capacity and, in turn, determine its malignant potential. Hence the present study was performed to evaluate the role of DWI and ADC in differentiating benign and malignant lesions and to determine other imaging features that can help in identifying neoplastic etiology.

This study was a hospital based observational study involving 43 subjects, with female subjects in the majority. The difference in the proportion of HPE findings between ADC values of the thyroid nodules was statistically significant (P-value <0.001). The ADC cut off value of 1.15 x 10^{-3} mm^2/s had a sensitivity of 87.50% in predicting final HPE malignancy. Specificity was 94.29%, and the total diagnostic accuracy was 93.02%. The ADC value of thyroid nodules had excellent predictive validity in predicting malignancy, as indicated by the area under the curve of 0.925 (P-value <0.001). Hence from our study results, the ADC value obtained had an excellent predictive value in predicting malignancy and correlated well with HPE diagnosis.

LIMITATIONS AND RECOMMENDATIONS:

- A small sample size of malignant lesions restricts the statistical power.
- Upgrading software of diffusion-weighted MR imaging in the future can aid in the recognition of smaller lesions in forthcoming studies.
- This study did not correlate ADC values with different histopathological subtypes of thyroid nodules due to the small sample size.

BIBLIOGRAPHY

REFERENCES:

1. Bhargava K, Narula H, Mittal A, Sharma D, Goel K, Nijhawan D. Role of Diffusion-Weighted Magnetic Resonance Imaging in Differentiating Benign From Malignant Thyroid Lesions: A Prospective Study. J Clin Diagnostic Res. 2020;14(4):1-4.
2. Wu Y, Yue X, Shen W, Du Y, Yuan Y, Tao X, et al. Diagnostic value of diffusion-weighted MR imaging in thyroid disease: application in differentiating benign from malignant disease. BMC Med Imaging. 2013;13:23.
3. Jemal A, Siegel R, Xu J, Ward E. Cancer statistics, 2010. CA Cancer J Clin. 2010;60(5):277-300.
4. Rosário PWS, Bessa B, Valadão MMA, Purisch S. Natural history of mild subclinical hypothyroidism: prognostic value of ultrasound. Thyroid. 2009;19(1):9-12.
5. McCoy KL, Jabbour N, Ogilvie JB, Ohori NP, Carty SE, Yim JH. The incidence of cancer and rate of false-negative cytology in thyroid nodules greater than or equal to 4 cm in size. Surgery. 2007;142(6):833-837.
6. Solbiati L, Osti V, Cova L, Tonolini M. Ultrasound of thyroid, parathyroid glands and neck lymph nodes. Eur Radiol. 2001;11(12):2411-2424.
7. Kim DW, Eun CK, In HS, Kim MH, Jung SJ, Bae SK. Sonographic differentiation of asymptomatic diffuse thyroid disease from normal thyroid: a prospective study. AJNR Am J Neuroradiol. 2010;31(10):1956-1960.
8. Kim DW. A comparative study of real-time and static ultrasonography diagnoses for the incidental detection of diffuse thyroid disease. Endocr Pract. 2015;21(8):910-916.
9. Pedersen OM, Aardal NP, Larssen TB, Varhaug JE, Myking O, Vik-Mo H. The value of ultrasonography in predicting autoimmune thyroid disease. Thyroid. 2000;10(3):251-259.
10. Kim DW, Lee YJ, Ahn HS, Baek HJ, Ryu JH, Kang T. Comparison of ultrasonography and computed tomography for diagnosing diffuse thyroid disease: a multicenter study. Radiol Med. 2018;123(7):515-523.
11. Kim DW, Jung SJ, Ha TK, Park HK, Kang T. Comparative study of ultrasound and computed tomography for incidentally detecting diffuse thyroid disease. Ultrasound Med Biol. 2014;40(8):1778-1784.
12. Ozturk T, Bozgeyik Z, Ozturk F, Burakgazi G, Akyol M, Coskun S, et al. The role of diffusion weighted MR imaging for differentiation between

Graves‟ disease and Hashimoto thyroiditis. Eur Rev Med Pharmacol Sci. 2015;19(15):2798-2803.

13. Abdel Razek AAK, Abd Allah SS, El-Said AAE-H. Role of Diffusion-Weighted Magnetic Resonance (MR) Imaging in Differentiation Between Graves‟ Disease and Painless Thyroiditis. Polish J Radiol. 2017;82:536-541.

14. Kang T, Kim DW, Lee YJ, Cho YJ, Jung SJ, Park HK, et al. Magnetic Resonance Imaging Features of Normal Thyroid Parenchyma and Incidental Diffuse Thyroid Disease: A Single-Center Study. Front Endocrinol (Lausanne). 2018;9:1-6.

15. Eida S, Sumi M, Sakihama N, Takahashi H, Nakamura T. Apparent diffusion coefficient mapping of salivary gland tumors: prediction of the benignancy and malignancy. AJNR Am J Neuroradiol. 2007;28(1):116-121.

16. Wang J, Takashima S, Takayama F, Kawakami S, Saito A, Matsushita T, et al. Head and neck lesions: characterization with diffusion-weighted echo-planar MR imaging. Radiology. 2001;220(3):621-630.

17. Gharib H, Papini E, Paschke R, Duick DS, Valcavi R, Hegedüs L, et al. American Association of Clinical Endocrinologists, Associazione Medici Endocrinologi, and European Thyroid Association Medical guidelines for clinical practice for the diagnosis and management of thyroid nodules: executive summary of recommendations. Endocr Pr. 2010;16(3):468-475.

18. Haugen BR, Alexander EK, Bible KC, Doherty GM, Mandel SJ, Nikiforov YE, et al. 2015 American Thyroid Association Management Guidelines for Adult Patients with Thyroid Nodules and Differentiated Thyroid Cancer: The American Thyroid Association Guidelines Task Force on Thyroid Nodules and Differentiated Thyroid Cancer. Thyroid. 2016;26(1):1-133.

19. Pinchot SN, Al-Wagih H, Schaefer S, Sippel R, Chen H. Accuracy of fine-needle aspiration biopsy for predicting neoplasm or carcinoma in thyroid nodules 4 cm or larger. Arch Surg. 2009;144(7):649-655.

20. Nachiappan AC, Metwalli ZA, Hailey BS, Patel RA, Ostrowski ML, Wynne DM. The thyroid: review of imaging features and biopsy techniques with radiologic-pathologic correlation. Radiographics. 2014;34(2):276-293.

21. Bozgeyik Z, Coskun S, Dagli AF, Ozkan Y, Sahpaz F, Ogur E. Diffusion-weighted MR imaging of thyroid nodules. Neuroradiology. 2009;51(3):193-198.

22. Erdem G, Erdem T, Muammer H, Mutlu DY, Firat AK, Sahin I, et al. Diffusion-weighted images differentiate benign from malignant thyroid nodules. J Magn Reson Imaging. 2010;31(1):94-100.

23. Peschmann A-L, Beer M, Ammann B, Dreyhaupt J, Kneer K, Beer AJ, et al. Quantitative DWI predicts event-free survival in children with neuroblastic tumours: preliminary findings from a retrospective cohort study. Eur Radiol Exp. 2019;3(1):6.

24. Lyng H, Haraldseth O, Rofstad EK. Measurement of cell density and necrotic fraction in human melanoma xenografts by diffusion weighted magnetic resonance imaging. Magn Reson Med. 2000;43(6):828-836.

25. Bujang MA, Adnan TH. Requirements for Minimum Sample Size for Sensitivity and Specificity Analysis. J Clin Diagn Res. 2016;10(10):YE01-YE06.

26. Ravikanth R, Selvam R, Pinto D. Role of quantitative diffusion-weighted magnetic resonance imaging in differentiating benign and malignant thyroid lesions. J Curr Res Sci Med. 2017;3(2):131.

27. Pemayun TGD. Current Diagnosis and Management of Thyroid Nodules. Acta Med Indones. 2016;48(3):247-257.

28. Bomeli SR, LeBeau SO, Ferris RL. Evaluation of a thyroid nodule. Otolaryngol Clin North Am. 2010;43(2):229-238, vii.

29. Durante C, Costante G, Lucisano G, Bruno R, Meringolo D, Paciaroni A, et al. The natural history of benign thyroid nodules. JAMA. 2015;313(9):926-935.

30. Netter, F.H. Atlas of Human Anatomy, 2nd Edition. Novartis Summit New Jersey; 1989. 514 p

31. Jacobsen B, VanKampen N, Ashurst JV. Anatomy, Head and Neck, Thyrohyoid Membrane. [Updated 2021 Jul 31]. In: StatPearls [Internet]. Treasure Island (FL): StatPearls Publishing; 2021. Available from: https://www.ncbi.nlm.nih.gov/books/NBK532995/

32. Roman BR, Randolph GW, Kamani D. Conventional Thyroidectomy in the Treatment of Primary Thyroid Cancer. Endocrinol Metab Clin North Am. 2019;48(1):125-141.

33. Allen E, Fingeret A. Anatomy, Head and Neck, Thyroid. [Updated 2021 Jul 26]. In: StatPearls [Internet]. Treasure Island (FL): StatPearls Publishing; 2021 Jan-. Available from: https://www.ncbi.nlm.nih.gov/books/NBK470452/.

34. Popoveniuc G, Jonklaas J. Thyroid nodules. Med Clin North Am.

2012;96(2):329-349.

35. Welker MJ, Orlov D. Thyroid nodules. Am Fam Physician. 2003;67(3):559-566.

36. Yeung MJ, Serpell JW. Management of the solitary thyroid nodule. Oncologist. 2008;13(2):105-112.

37. Dean DS, Gharib H. Epidemiology of thyroid nodules. Best Pract Res Clin Endocrinol Metab. 2008;22(6):901-911.

38. Cohen A, Rovelli A, Merlo DF, van Lint MT, Lanino E, Bresters D, et al. Risk for secondary thyroid carcinoma after hematopoietic stem-cell transplantation: an EBMT Late Effects Working Party Study. J Clin Oncol. 2007;25(17):2449-2454.

39. Vanderpump MP, Tunbridge WM, French JM, Appleton D, Bates D, Clark F, et al. The incidence of thyroid disorders in the community: a twenty-year follow-up of the Whickham Survey. Clin Endocrinol (Oxf). 1995;43(1):55-68.

40. Belfiore A, La Rosa GL, La Porta GA, Giuffrida D, Milazzo G, Lupo L, et al. Cancer risk in patients with cold thyroid nodules: relevance of iodine intake, sex, age, and multinodularity. Am J Med. 1992;93(4):363-369.

41. Kameyama K, Ito K, Takami H. [Pathology of benign thyroid tumor]. Nihon Rinsho. 2007;65(11):1973-1978.

42. Saad AG, Kumar S, Ron E, Lubin JH, Stanek J, Bove KE, et al. Proliferative activity of human thyroid cells in various age groups and its correlation with the risk of thyroid cancer after radiation exposure. J Clin Endocrinol Metab. 2006;91(7):2672-2677.

43. Cibas ES, Ali SZ. The 2017 Bethesda System for Reporting Thyroid Cytopathology. Thyroid. 2017;27(11):1341-1346.

44. Nikiforov YE, Seethala RR, Tallini G, Baloch ZW, Basolo F, Thompson LDR, et al. Nomenclature Revision for Encapsulated Follicular Variant of Papillary Thyroid Carcinoma: A Paradigm Shift to Reduce Overtreatment of Indolent Tumors. JAMA Oncol. 2016;2(8):1023-1029.

45. Gharib H, Papini E. Thyroid nodules: clinical importance, assessment, and treatment. Endocrinol Metab Clin North Am. 2007;36(3):707-735, vi.

46. Alexander EK, Heering JP, Benson CB, Frates MC, Doubilet PM, Cibas ES, et al. Assessment of nondiagnostic ultrasound-guided fine needle aspirations of thyroid nodules. J Clin Endocrinol Metab. 2002;87(11):4924-4927.

47. Singh RS, Wang HH. Timing of repeat thyroid fine-needle aspiration in the management of thyroid nodules. Acta Cytol. 2011;55(6):544-548.

48. Lin S-T, Tseng F-Y, Hsu C-J, Yeh T-H, Chen Y-S. Thyroglossal duct cyst: a comparison between children and adults. Am J Otolaryngol. 2008;29(2):83-87.

49. Eustatia-Rutten CFA, Corssmit EPM, Biermasz NR, Pereira AM, Romijn JA, Smit JW. Survival and death causes in differentiated thyroid carcinoma. J Clin Endocrinol Metab. 2006;91(1):313-319.

50. Leboulleux S, Rubino C, Baudin E, Caillou B, Hartl DM, Bidart J-M, et al. Prognostic factors for persistent or recurrent disease of papillary thyroid carcinoma with neck lymph node metastases and/or tumor extension beyond the thyroid capsule at initial diagnosis. J Clin Endocrinol Metab. 2005;90(10):5723-5729.

51. Grover VPB, Tognarelli JM, Crossey MME, Cox IJ, Taylor-Robinson SD, McPhail MJW. Magnetic Resonance Imaging: Principles and Techniques: Lessons for Clinicians. J Clin Exp Hepatol. 2015;5(3):246-255.

52. Geethanath S, Vaughan JT. Accessible magnetic resonance imaging: A review. J Magn Reson Imaging. 2019;49(7):e65-e77.

53. Koh D-M, Collins DJ. Diffusion-weighted MRI in the body: applications and challenges in oncology. AJR Am J Roentgenol. 2007;188(6):1622-1635.

54. Kwee TC, Takahara T, Ochiai R, Katahira K, Van Cauteren M, Imai Y, et al. Whole-body diffusion-weighted magnetic resonance imaging. Eur J Radiol. 2009;70(3):409-417.

55. Neil JJ. Diffusion imaging concepts for clinicians. J Magn Reson Imaging. 2008;27(1):1-7.

56. Malayeri AA, El Khouli RH, Zaheer A, Jacobs MA, Corona-Villalobos CP, Kamel IR, et al. Principles and Applications of Diffusion-weighted Imaging in Cancer Detection, Staging, and Treatment Follow-up. RadioGraphics. 2011;31(6):1773-1791.

57. Linh LT, Cuongq NN, Hung TV, Hieu N Van, Lenh B Van, Hue ND, et al. Value of diffiusion weighted MRI with quantitative ADC map in diagnosis of malignant thyroid disease. Diagnostics. 2019;9(4):129.

58. Razek AAKA, Sadek AG, Kombar OR, Elmahdy TE, Nada N. Role of apparent diffusion coefficient values in differentiation between malignant and benign solitary thyroid nodules. AJNR Am J Neuroradiol. 2008;29(3):563-568.

59. Shokry AM, Hassan TA, Baz AA, Ahmed ASO, Zedan MH. Role of diffusion weighted magnetic resonance imaging in differentiation of benign and malignant thyroid nodules. Egypt J Radiol Nucl Med. 2018;49(4):1014-1021.

60. Henzler T, Schmid-Bindert G, Schoenberg SO, Fink C. Diffusion and perfusion MRI of the lung and mediastinum. Eur J Radiol. 2010;76(3):329-336.

61. Elshafey R, Elattar A, Mlees M, Esheba N. Role of quantitative diffusion-weighted MRI and 1H MR spectroscopy in distinguishing between benign and malignant thyroid nodules. Egypt J Radiol Nucl Med. 2014;45(1):89-96.

62. Levison D, Reid R, Burt AD, Harrison DJ, Fleming S. Muir"s Textbook of Pathology. CRC Press; 2012.

63. Abdel Razek AAK, Soliman NY, Elkhamary S, Alsharaway MK, Tawfik A. Role of diffusion-weighted MR imaging in cervical lymphadenopathy. Eur Radiol. 2006;16(7):1468-1477.

64. Schueller-Weidekamm C, Kaserer K, Schueller G, Scheuba C, Ringl H, Weber M, et al. Can quantitative diffusion-weighted MR imaging differentiate benign and malignant cold thyroid nodules? Initial results in 25 patients. AJNR Am J Neuroradiol. 2009;30(2):417-422.

65. Schueller-Weidekamm C, Schueller G, Kaserer K, Scheuba C, Ringl H, Weber M, et al. Diagnostic value of sonography, ultrasound-guided fine-needle aspiration cytology, and diffusion-weighted MRI in the characterization of cold thyroid nodules. Eur J Radiol. 2010;73(3):538-544.

66. Herneth AM, Guccione S, Bednarski M. Apparent diffusion coefficient: a quantitative parameter for in vivo tumor characterization. Eur J Radiol. 2003;45(3):208-213.

67. Delorme S, Knopp M V. Non-invasive vascular imaging: assessing tumour vascularity. Eur Radiol. 1998;8(4):517-527.

68. A. Fath El- Bab H, M. Deabes S, H. El-Shafey M, M. Nafady H. Rrole of diffusion-weighted mr imaging of thyroid nodules. Al-Azhar Med J. 2021;50(1):521-532.

69. Huang S, Cai W, Han S, lin Y, Wang Y, Chen F, et al. Differences in the dielectric properties of various benign and malignant thyroid nodules. Med Phys. 2021;48(2):760-769.

70. Abdelgawad EA, AbdelGawad EA, AbuElCebaa O, Atiya AM. Can

quantitative diffusion-weighted MR imaging differentiate between different subtypes of benign and malignant solitary thyroid nodules? Egypt J Radiol Nucl Med 2020 511. 2020;51(1):1-6.

71. MONA AA, MAHA A, SHERIF A. Diffusion Weighted Magnetic Resonance Imaging in Differentiation of Benign and Malignant Thyroid Nodules. Med J Cairo Univ. 2020;88(12):2183-2191.

72. Kong W, Yue X, Ren J, Tao X. A comparative analysis of diffusion-weighted imaging and ultrasound in thyroid nodules. BMC Med Imaging. 2019;19(1):1-6.

73. Aghaghazvini L, Sharifian H, Yazdani N, Hosseiny M, Kooraki S, Pirouzi P, et al. Differentiation between benign and malignant thyroid nodules using diffusion-weighted imaging, a 3-T MRI study. Indian J Radiol Imaging. 2018;28(4):460-464.

74. Ekinci O, Boluk SE, Eren T, Ozemir IA, Boluk S, Salmaslioglu A, et al. Diffusion-weighted magnetic resonance imaging for the detection of thyroid cancer. Cir Esp. 2018;96(10):620-626.

75. Abdel-Rahman HM, Abowarda MH, Abdel-Aal SM. Diffusion-weighted MRI and apparent diffusion coefficient in differentiation of benign from malignant solitary thyroid nodule. Egypt J Radiol Nucl Med. 2016;47(4):1385-1390.

76. Chen L, Chen L, Xu J, Bao J, Huang X, Hu X, et al. Diffusion-weighted MRI in differentiating malignant from benign thyroid nodules: a meta-analysis. BMJ Open. 2016;6(1):e008413.

77. Abd el Aziz LM, Hamisa M, Badwy ME. Differentiation of thyroid nodules using diffusion-weighted MRI. Alexandria J Med. 2015;51(4):305-309.

78. Wu LM, Chen XX, Li YL, Hua J, Chen J, Hu J, et al. On the utility of quantitative diffusion-weighted MR imaging as a tool in differentiation between malignant and benign thyroid nodules. Acad Radiol. 2014;21(3):355-363.

79. Shi HF, Feng Q, Qiang JW, Li RK, Wang L, Yu JP. Utility of diffusion-weighted imaging in differentiating malignant from benign thyroid nodules with magnetic resonance imaging and pathologic correlation. J Comput Assist Tomogr. 2013;37(4):505-510.

80. Mutlu H, Sivrioglu AK, Sonmez G, Velioglu M, Sildiroglu HO, Basekim CC, et al. Role of apparent diffusion coefficient values and diffusion-weighted magnetic resonance imaging in differentiation between benign and malignant thyroid nodules. Clin Imaging. 2012;36(1):1-7.

81. Dilli A, Ayaz UY, Cakir E, Cakal E, Gultekin SS, Hekimoglu B. The efficacy of apparent diffusion coefficient value calculation in differentiation between malignant and benign thyroid nodules. Clin Imaging. 2012;36(4):316-322.

82. IBM Corp. Released 2013. IBM SPSS Statistics for Windows, Version 22.0. Armonk, NY: IBM Corp.

83. Rho MH, Kim DW. Computed tomography features of incidentally detected diffuse thyroid disease. Int J Endocrinol. 2014;2014.

84. Anderson J. Tumors: General features, types and examples. In: Anderson JR, editor. Muir‟s Textbook of Pathology. London: Edward Arnold; 1992. pp. 127–56.

85. Khizer AT, Raza S. Diffusion-weighted MR imaging and ADC mapping in differentiating benign from malignant thyroid nodules. J Coll Physicians Surg Pakistan. 2015;25(11):785-789.

86. Nakahira M, Saito N, Murata S, Sugasawa M, Shimamura Y, Morita K, et al. Quantitative diffusion-weighted magnetic resonance imaging as a powerful adjunct to fine needle aspiration cytology for assessment of thyroid nodules. Am J Otolaryngol. 2012;33(4):408-416.

87. Ilica AT, Artaş H, Ayan A, Günal A, Emer O, Kilbas Z, et al. Initial experience of 3 tesla apparent diffusion coefficient values in differentiating benign and malignant thyroid nodules. J Magn Reson Imaging. 2013;37(5):1077-1082.

ANNEXURE

SRI DEVARAJ URS ACADEMY OF HIGHER EDUCATION AND RESEARCH, TAMAKA, KOLAR, KARNATAKA

ANNEXURE I - PATIENT PROFORMA

"ROLE OF DIFFUSION WEIGHTED MRI IN DIFFERENTIATING BENIGN FROM MALIGNANT THYROID NODULES"

DEMOGRAPHIC DETAILS:

- **Name:**
- **Age:**
- **Sex :**
- **UHID:**

CLINICAL HISTORY:

MRI FINDINGS:

- **Side of involvement :**
- **Number of nodules :**
- **Size of the nodule considered :**
- **Shape of the nodule considered :**
- **Signal characteristics :**

T1	T2	Restricting/non-restricting	ADC Value

- **Extrathyroidal invasion :**
- **Calcifications :**
- **Lymph nodes :**

PATHOLOGICAL FINDINGS:

FINAL DIAGNOSIS:

SRI DEVARAJ URS ACADEMY OF HIGHER EDUCATION AND RESEARCH, TAMAKA, KOLAR, KARNATAKA

INFORMED CONSENT FORM

STUDYTITLE: **ROLE OF DIFFUSION WEIGHTED MRI IN DIFFERENTIATING BENIGN FROM MALIGNANT THYROID NODULES**

CHIEF RESEARCHER/ PG GUIDE"S NAME: Dr. N. RACHEGOWDA

PRINCIPAL INVESTIGATOR: Dr. MONISHA V.

NAME OF THE SUBJECT:

AGE :

GENDER :

a. I have been informed in my own language that this study involves MRI as part of procedure. I have been explained thoroughly and understand the procedure.
b. I understand that the medical information produced by this study will become part of institutional record and will be kept confidential by the said institute.
c. I understand that my participation is voluntary and may refuse to participate or may withdraw my consent and discontinue participation at any time without prejudice to my present or future care at this institution.
d. I agree not to restrict the use of any data or results that arise from this study provided such a use is only for scientific purpose(s).
e. I confirm that Dr. RACHEGOWDA N. / Dr. MONISHA V. (chief researcher/ name of PG

guide/name of the principal investigator) has explained to me the purpose of research and the study procedure that I will undergo and the possible risks and discomforts that I may experience, in my own language. I hereby agree to give valid consent to participate as a subject in this research project.

Participant's signature/thumb impression

Signature of the witness: Date:

1)

2)

I have explained to_____(subject) the purpose of the research, the possible risk and benefits to the best of my ability.

Chief Researcher/ Guide signature Date:

SRI DEVARAJ URS ACADEMY OF HIGHER EDUCATION AND RESEARCH, TAMAKA, KOLAR, KARNATAKA

PATIENT INFORMATION SHEET

Principal Investigator: Dr. Monisha V. / Dr. N. Rachegowda

I, Dr. MONISHA V, post-graduate student in Department of Radio-Diagnosis at Sri Devaraj Urs Medical College, will be conducting a study titled "ROLE OF DIFFUSION WEIGHTED MRI IN DIFFERENTIATING BENIGN FROM MALIGNANT THYROID NODULES" for my dissertation under the guidance of Dr. Rache Gowda N, Professor, Department of Radio-Diagnosis. In this study, we will assess the diagnostic potential of Diffusion weighted imaging in differentiating benign from malignant thyroid nodules. You would have undergone MRI before entering the study. You will not be paid any financial compensation for participating in this research project.

All of your personal data will be kept confidential and will be used only for research purpose by this institution. You are free to participate in the study. You can also withdraw from the study at any point of time without giving any reasons whatsoever. Your refusal to participate will not prejudice you to any present or future care at this institution

Name and Signature of the Principal Investigator

Date

MASTER CHART

MASTER CHART

SL NO	UHIDNO	AGE	SEX	SIDE Lobe OF INVOLVEMENT	Number	SIZE	SHAPE	SIGNAL INTENSITYT1	SIGNAL INTENSITYT2	Margins	Composition of the lesion
1	7,85,597	30	F	Left	One	2.4 x 2.0 cm	Irregular	isointense	Heterogeneously hyperintense	Irregular	Solid
2	7,68,710	38	F	Right	One	0.8 x 0.7 cm	Round	iso	iso	Smooth	Predominantly cystic
3	7,89,719	50	F	Both	Multiple	1.7 x 1.5 cm	Round	iso	iso	Smooth	Predominantly solid
4	7,62,900	40	F	Right	One	3.1 x 2.8 cm	Round	iso	iso	Smooth	Solid-cystic
5	7,65,854	50	F	Right	One	1.2 x 0.9 cm	Round	iso	Hetero hyper	Smooth	Solid-cystic
6	8,51,825	38	F	Right	One	1.0 x 0.9 cm	Round	iso	Hetero hyper	Smooth	Solid-cystic
7	8,52,623	78	M	Left	Multiple	1.0 x 0.7 cm	Irregular	iso	Hetero hyper	Irregular	Predominantly solid
8	8,44,120	65	M	Left	One	1.3 x 0.7 cm	Round	iso	Hetero hyper	Smooth	Predominantly solid
9	8,56,282	36	F	Right	One	2.8 x 2.1 cm	Oval	iso	Hetero hyper	Lobulated	Solid-cystic
10	8,54,212	45	F	Left	One	1.4 x 1.3 cm	Round	iso	iso	Smooth	Predominantly solid
11	8,81,333	45	F	Right	One	4.3 x 2.4 cm	Round	iso	Hetero hyper	Smooth	Predominantly solid
12	8,81,345	24	F	Right	One	4.2 x 4.1 cm	Round	iso	Hetero hyper	Smooth	Solid
13	8,81,313	50	F	ISTHMUS	One	1.8 x 1.5 cm	Round	iso	Hetero hyper	Smooth	Solid-cystic
14	8,76,333	65	F	BOTH(largest on right + isthmus)	Multiple	2.0 X 1.0 cm	Round	iso	Hetero hyper	Smooth	Solid-cystic
15	8,65,223	58	F	Left	One	11.5 X 7.5 cm	Irregular	iso	Hetero hyper	Irregular	Predominantly solid
16	8,82,534	45	M	Left	Multiple	3.1 x 3.0 cm	Round	iso	Hetero hyper	Smooth	Predominantly solid
17	8,88,482	55	F	Both	Multiple	2.0 x 1.5 cm	Oval	iso	Hetero hyper	Smooth	Solid-cystic
18	8,81,455	50	F	Right	One	3.5 x 3.3 cm	Round	Hyper	Hypo	Smooth	Predominantly cystic
19	8,85,207	50	F	Right	One	1.4 X 0.8 cm	Oval	iso	Hetero hyper	Smooth	Solid
20	8,69,549	40	F	Left	One	2.9 x 1.8 cm	Oval	iso	Hetero hyper	Smooth	Solid
21	8,77,786	55	M	Left	Multiple	2.8 x 1.3 cm	Oval	iso	Hetero hyper	Smooth	Solid
22	8,78,242	65	F	Both	Multiple	5.6 x 4.8 cm	Irregular	iso	Hetero hyper	Irregular	Solid
23	8,67,449	40	F	Left	One	8.4 x 6.9 cm	Irregular	iso	Hetero hyper	Irregular	Solid
24	8,62,190	29	F	Both	Two	1.9 x 1.3 cm	Irregular	iso	Hetero hyper	Irregular	Solid
25	8,95,108	25	F	Both	Multiple	2.7 x 2.4 cm	Round	iso	Hetero hyper	Smooth	Solid
26	8,95,985	55	M	Right	Two	2.8 x 2.5 cm	Round	iso	Hetero hyper	Smooth	Solid
27	8,99,690	41	F	Right	One	1.2 x 0.9 cm	Round	iso	Hetero hyper	Smooth	Solid
28	9,02,416	25	F	Both	Multiple	3.4 X 2.8 cm	Round	mixed	mixed	Smooth	Solid-cystic
29	9,06,964	62	M	Left	Two	1.2 x 0.8 cm	Oval	iso	Hetero hyper	Smooth	Solid

30	9,10,330	73	F	Right	One	2.5 x 1.2 cm	Oval	iso	Hetero hyper	Smooth	Solid
31	9,08,762	55	F	Left	One	2.1 x 1.4 cm	Oval	iso	Hetero hyper	Smooth	Solid
32	9,11,633	56	F	Both	Two	2.2 x 1.0 cm	Oval	iso	Hetero hyper	Smooth	Solid
33	9,16,706	55	F	Both	Two	2.0 x 1.5 cm	Round	iso	Hetero hyper	Lobulated	Solid-cystic
34	9,22,616	72	M	Left	One	3.1 x 2.9 cm	Round	iso	Hetero hyper	Smooth	Solid
35	9,23,145	45	M	Left	One	3.5 x 3.2	Round	iso	Hetero hyper	Smooth	Solid
36	9,24,837	46	F	Left	One	3.7 x 2.7 cm	Oval	iso	Hetero hyper	Smooth	Solid
37	9,23,931	78	F	Both	Multiple	1.7 x 1.0 cm	Oval	iso	Hetero hyper	Smooth	Predominantly solid
38	9,09,580	30	F	Left	Multiple	1.2 x 0.8 cm	Round	iso	Hetero hyper	Smooth	Solid
39	92,433	60	F	Both lobes & isthmus	Multiple	3.0 x 2.4	Round	iso	Hetero hyper	Smooth	Solid
40	9,25,642	63	F	Both	Multiple	3.3 x 3.1 cm	Round	iso	Hetero hyper	Smooth	Predominantly cystic
41	9,27,907	35	F	Left	One	5.0 x 3.1 cm	Oval	iso	Hetero hyper	Smooth	Solid
42	9,23,145	60	F	Right	One	3.5 x 3.1 cm	Round	iso	Hetero hyper	Smooth	Solid
43	9,87,609	68	F	Both	Multiple	2.5 x 2.0 cm	Round	iso	Hetero hyper	Smooth	Solid

SL NO	Extra thyroid alextension	Calcifications	Lymph nodes	DWI	ADC	Pathological findings	HPE	MRI findings
1	Nil	Nil	Nil	R	0.89	Papillary thyroid carcinoma	Malignant	M
2	Nil	Nil	Nil	NR	1.30	Nodular hyperplasia with secondary changes - Bethesda category type II	Benign	B
3	Nil	Nil	Nil	NR	1.30	Hashimoto's thyroiditis	Benign	B
4	Nil	Nil	Present	NR	1.60	Nodular hyperplasia	Benign	B
5	Nil	Nil	Nil	NR	1.80	Nodular hyperplasia - Bethesda category type II	Benign	B
6	Nil	Nil	Nil	NR	1.30	Nodular hyperplasia	Benign	B
7	Nil	Present	Present	R	0.71	Papillary thyroid carcinoma	Malignant	M
8	Nil	Present	Present	R	0.90	Follicular carcinoma	Malignant	M
9	Nil	Nil	Present	R	1.10	Hyalinizing trabecular adenoma	Benign	B
10	Nil	Nil	Nil	NR	1.40	Hashimoto's thyroiditis	Benign	B
11	Nil	Nil	Nil	NR	1.40	Lymphocytic thyroiditis	Benign	B
12	Nil	Nil	Nil	NR	1.90	Lymphocytic thyroiditis	Benign	B
13	Nil	Nil	Nil	NR	2.20	Nodular hyperplasia	Benign	B
14	Nil	Nil	Nil	NR	1.90	Nodular hyperplasia	Benign	B
15	Retrosternal	Present	Nil	R	1.00	Anaplastic carcinoma	Malignant	M
16	Nil	Present	Nil	NR	1.90	Benign follicular lesion	Benign	B
17	Nil	Nil	Nil	NR	1.40	Hashimoto's thyroiditis	Benign	B
18	Nil	Nil	Nil	NR	1.40	Colloid nodule	Benign	B
19	Nil	Nil	Nil	NR	1.40	Colloid nodule	Benign	B
20	Nil	Nil	Nil	NR	2.90	Colloid nodule	Benign	B
21	Nil	Nil	Present	R	1.10	Papillary carcinoma	Malignant	M
22	Nil	Nil	Nil	R	1.70	Adenomatoid nodule with cystic change	Benign	B
23	Nil	Nil	Nil	NR	1.50	Minimally invasive follicular carcinoma (hurthle cell type)	Malignant	M
24	Nil	Nil	Nil	NR	1.10	Benign follicular lesion	Benign	B
25	Nil	Nil	Nil	NR	1.20	Lymphocytic thyroiditis	Benign	B
26	Nil	Nil	Nil	NR	1.60	Hashimoto's thyroiditis	Benign	B
27	Nil	Nil	Nil	NR	1.40	Lymphocytic thyroiditis	Benign	B
28	Nil	Nil	Nil	NR	1.60	Benign follicular lesion - colloid goitre	Benign	B
29	Nil	Nil	Present	NR	1.80	Lymphocytic thyroiditis	Benign	B
30	Nil	Nil	Nil	NR	0.90	Nodular hyperplasia	Benign	B
31	Nil	Nil	Present	NR	1.80	Lymphocytic thyroiditis	Benign	B

32	Nil	Nil	Nil	NR	0.90	Benign follicular lesion	Benign	B
33	Nil	Nil	Nil	NR	1.80	Nodular hyperplasia	Benign	B
34	Nil	Present	Present	R	0.90	Papillary thyroid carcinoma - Bethesda category V,Metastatic deposits of papillary thyroid	Malignant	M
35	Nil	Nil	Nil	NR	2.10	Nodular hyperplasia	Benign	B
36	Nil	Nil	Nil	NR	1.60	Colloid goitre - Left thyroid	Benign	B
37	Nil	Nil	Present	R	0.92	Anaplastic carcinoma thyroid	Malignant	M
38	Nil	Nil	Nil	NR	1.40	Nodular hyperplasia	Benign	B
39	Nil	Nil	Nil	NR	1.10	Lymphocytic thyroiditis	Benign	B
40	Nil	Nil	Nil	NR	1.60	Colloid goitre	Benign	B
41	Nil	Nil	Nil	NR	1.40	Nodular hyperplasia	Benign	B
42	Nil	Nil	Nil	NR	1.10	Benign follicular lesion	Benign	B
43	Nil	Nil	Nil	NR	1.70	Hashimoto's thyroiditis	Benign	B

DWI MRI WITH ADC VALUES OF FEW OF MY CASES

Malignant restricting nodule

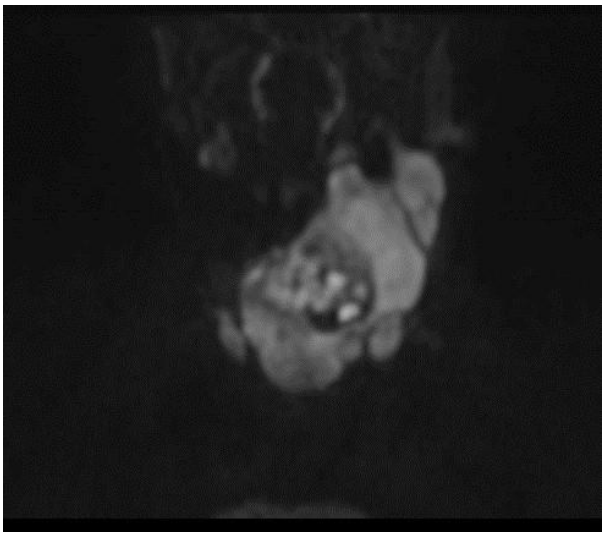

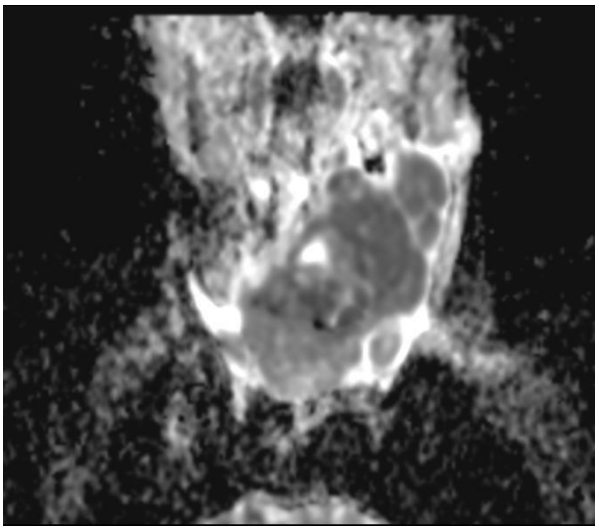

A 58-year-old female presented with a large swelling in the neck. MRI diffusion weighted imaging at *b value 800* coronal section – shows a large heterogeneously hyperintense lesion arising from left lobe of thyroid with corresponding area showing signal drop on ADC – suggestive of restricted diffusion on DWI with ADC. Mean ADC value obtained was 0.77 x 10^{-3} mm^2/s. FNAC revealed features suggestive of anaplastic carcinoma thyroid.

Malignant non-restricting nodule

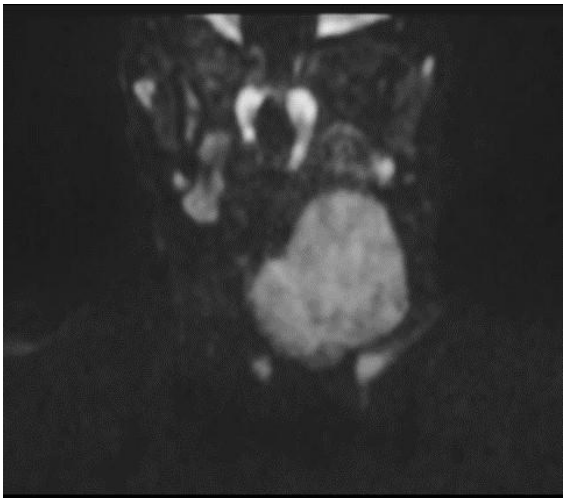

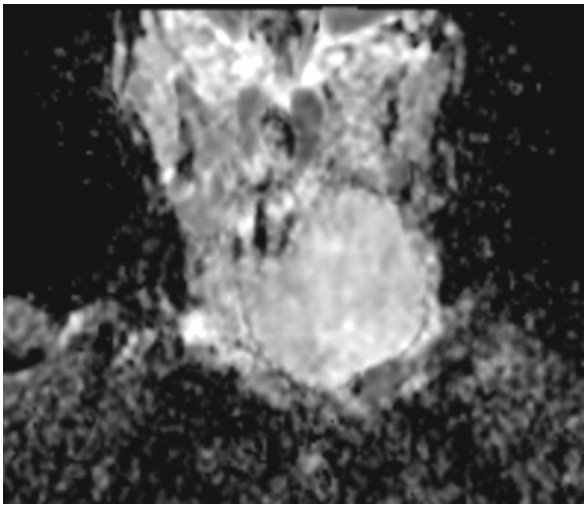

A 40-year-old female presented with a large swelling in the neck. MRI diffusion weighted imaging at b value 800 coronal section – shows a large heterogeneously hyperintense lesion arising from left lobe of thyroid with no evidence of restricted diffusion on ADC. Mean ADC value obtained was 0.8 x 10-3 mm^2/s. FNAC revealed features suggestive of minimally invasive follicular carcinoma thyroid.

Benign restricting nodule

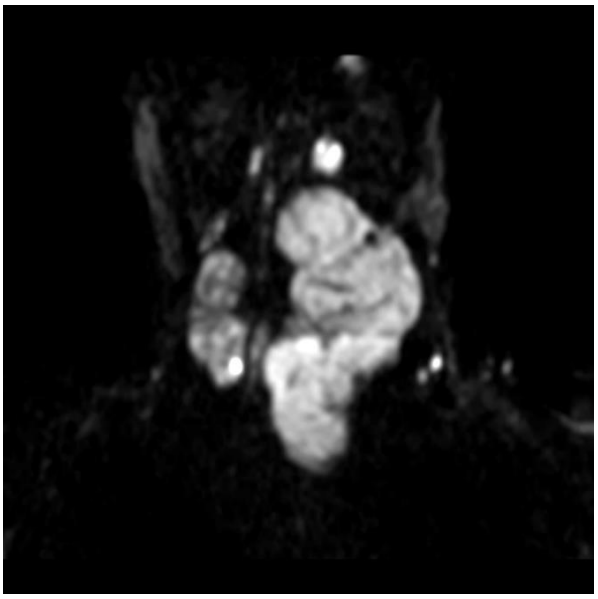
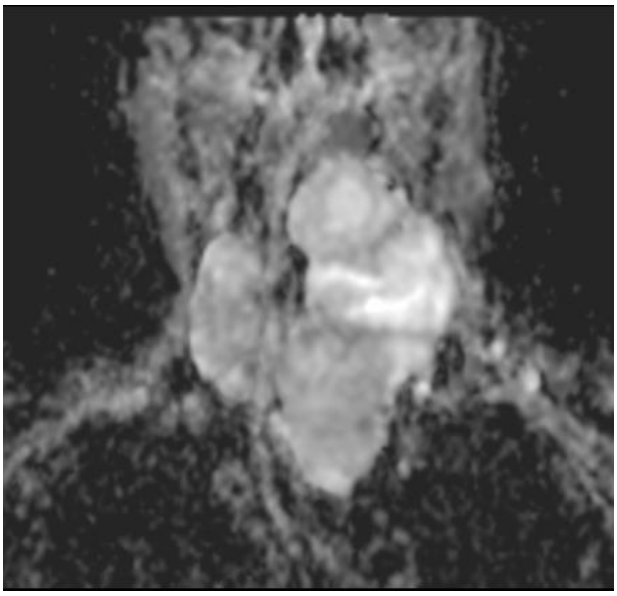

A 65-year-old female presented with a swelling in the neck. MRI diffusion weighted imaging at *b value 800* coronal section – shows multiple heterogeneously hyperintense lesions arising from both lobes of thyroid with patchy areas of restricted diffusion on ADC. Mean ADC value obtained was 1.7 x 10^{-3} mm^2/s. FNAC revealed features suggestive of adenomatoid nodule, a benign entity.

Benign non-restricting nodule


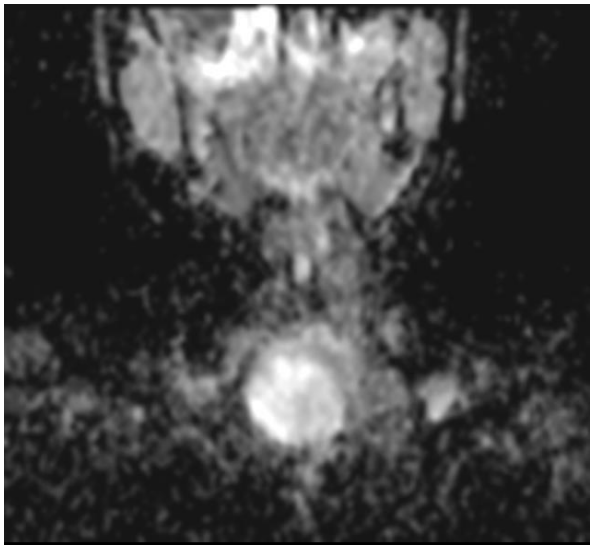

A 24-year-old female presented with swelling in the neck. MRI diffusion weighted imaging at b value 800 coronal section – shows a heterogeneously hyperintense lesion arising from right lobe of thyroid with no evidence of restricted diffusion on ADC. Mean ADC value obtained was 1.9 x 10-3 mm^2/s. FNAC revealed features suggestive of lymphocytic thyroiditis.